

## Phytoplankton growth formulation in marine ecosystem models: Should we take into account photo-acclimation and variable stoichiometry in oligotrophic areas?

S.-D. Ayata<sup>a, b, c, \*</sup>, M. Lévy<sup>b</sup>, O. Aumont<sup>d</sup>, A. Sciandra<sup>a</sup>, J. Sainte-Marie<sup>c, f</sup>, A. Tagliabue<sup>g</sup>,  
O. Bernard<sup>a, e</sup>

<sup>a</sup> LOV, UMR 7093, B.P. 28, 06234 Villefranche-sur-mer, France

<sup>b</sup> LOCEAN-IPSL, CNRS/UPMC/IRD/MNH, 4 place Jussieu, 75005 Paris, France

<sup>c</sup> BANG, INRIA Paris-Rocquencourt, BP 105, 78153 Le Chesnay Cedex, France

<sup>d</sup> LPO, CNRS/IFREMER/UBO, BP 70, 29280 Plouzané, France

<sup>e</sup> BIOCORE, INRIA, B.P. 93, 06902 Sophia-Antipolis Cedex, France

<sup>f</sup> Laboratoire Saint-Venant, 6 quai Watier, 78401 Chatou Cedex, France

<sup>g</sup> Dept. of Earth, Ocean and Ecological Sciences, School of Environmental Sciences, University of Liverpool, 4 Brownlow Street, Liverpool L69 3GP, United Kingdom

\*: Corresponding author : S.-D. Ayata, email address : [sakina.ayata@normalesup.org](mailto:sakina.ayata@normalesup.org)

### Abstract:

The aim of this study is to evaluate the consequences of accounting for variable Chl:C (chlorophyll:carbon) and C:N (carbon:nitrogen) ratios in the formulation of phytoplankton growth in biogeochemical models. We compare the qualitative behavior of a suite of phytoplankton growth formulations with increasing complexity: 1) a Redfield formulation (constant C:N ratio) without photo-acclimation (constant Chl:C ratio), 2) a Redfield formulation with diagnostic chlorophyll (variable and empirical Chl:C ratio), 3) a quota formulation (variable C:N ratio) with diagnostic chlorophyll, and 4) a quota formulation with prognostic chlorophyll (dynamic variable). These phytoplankton growth formulations are embedded in a simple marine ecosystem model in a 1D framework at the Bermuda Atlantic Time-series (BATS) station. The model parameters are tuned using a stochastic assimilation method (micro-genetic algorithm) and skill assessment techniques are used to compare results. The lowest misfits with observations are obtained when photo-acclimation is taken into account (variable Chl:C ratio) and with non-Redfield stoichiometry (variable C:N ratio), both under spring and summer conditions. This indicates that the most flexible models (i.e., with variable ratios) are necessary to reproduce observations. As seen previously, photo-acclimation is essential in reproducing the observed deep chlorophyll maximum and subsurface production present during summer. Although Redfield and quota formulations of C:N ratios can equally reproduce chlorophyll data the higher primary production that arises from the quota model is in better agreement with observations. Under the oligotrophic conditions that typify the BATS site no clear difference was detected between quota formulations with diagnostic or prognostic chlorophyll.

## Highlights

► We compare phytoplankton growth formulations with increasing complexity, after tuning through microgenetic algorithm. ► The most flexible models, i.e., with variable ratios, are necessary to reproduce observations under oligotrophic regimes. ► Photo-acclimation (variable Chl:C) is needed to reproduce the subsurface chlorophyll maximum in summer. ► Non-Redfield stoichiometry (variable C:N) is needed to simulate more realistic primary production estimates. ► No clear difference is detected between quota (non-Redfield) formulations with diagnostic or prognostic chlorophyll.

**Keywords:** Biogeochemical modeling ; Phytoplankton ; Photo-acclimation ; Redfield ratio ; Internal quota ; BATS ; Optimization ; Micro-genetic algorithm

## 1. Introduction

---

During the last twenty years, marine ecosystem (or biogeochemical) models have been widely used to study the response of primary production to perturbation of the physical environment along a wide range of temporal and spatial scales. Most of these models follow the same general structure: they use nitrogen as the main currency, and account for a simplified food-web

7 which generally includes phytoplankton and zooplankton, and a regeneration  
8 network with detritus, dissolved organic nitrogen, and various nutrients (i.e.,  
9 Fasham et al., 1990). Whereas the complexity of marine biogeochemical mod-  
10 els has increased in the last decade (reaching sometimes about eighty state  
11 variables as in Follows et al., 2007), simple phytoplankton growth models are  
12 still usually embedded within these ecosystem models, with strong simplifica-  
13 tions on phytoplankton physiology, such as using constant C:N stoichiometry  
14 or not accounting for photo-acclimation (using constant Chl:C ratio).

15 Phytoplankton growth formulations involving different complexities in  
16 the representation of physiological processes (such as photosynthesis, nutri-  
17 ent uptake, photo-acclimation, or energy storage) have been derived from  
18 laboratory experiments (Zonneveld, 1998; Baklouti et al., 2006). However,  
19 directly transposing the relationships derived from these laboratory exper-  
20 iments, which generally involve a single phytoplankton species and explore  
21 a limited set of forcing conditions (nutrient supply, temperature, light), to  
22 global marine ecosystem models is not straightforward and is currently the  
23 subject of some debates (Flynn, 2003a; Franks, 2009; Flynn, 2010; Anderson,  
24 2010).

25 The simplest phytoplanktonic growth formulations use a classical Michaelis-  
26 Menten representation of nutrient uptake (Monod, 1949, 1950) and assume  
27 constant stoichiometry between carbon, nitrogen and phosphorus (Redfield  
28 et al., 1963). In these models, phytoplankton are represented by a single state  
29 variable, the phytoplankton biomass, expressed in nitrogen, phosphorus or  
30 carbon currency. Because of their relative simplicity, these models are gen-  
31 erally used for global scale studies (Aumont and Bopp, 2006; Follows et al.,

2007; Dutkiewicz et al., 2009). More sophisticated formulations, inspired from the original work of Droop (1968, 1983), explicitly account for the dynamics of internal quotas of phytoplanktonic cells (Flynn, 2008; Klausmeier et al., 2004; Bougaran et al., 2010; Mairet et al., 2011; Bernard, 2011). In these formulations, phytoplankton are represented by at least two variables, usually the phytoplankton biomass in both carbon and nitrogen currency. This allows to decouple the dynamics of nutrient uptake from carbon fixation, depending on the physiological state of phytoplankton. Various versions of such formulations have been successfully applied to 1D marine ecosystem models (Lancelot et al., 2000; Allen et al., 2002; Lefèvre et al., 2003; Mongin et al., 2003; Blackford et al., 2004; Salihoglu et al., 2008) and also attempted in 3D ecosystem models (Tagliabue and Arrigo, 2005; Vichi et al., 2007; Vichi and Masina, 2009; Vogt et al., 2010).

The dynamics of pigment contents, most frequently of chlorophyll *a* (Chl), can also be represented with different levels of complexity. The Chl:C ratios can either be constant (no photo-acclimation), diagnostic (from an empirical (Cloern et al., 1995; Bernard, 2011) or a mechanistic (Geider and Platt, 1986; Doney et al., 1996; Bissett et al., 1999) static relationship), or prognostic (i.e., with a dynamic evolution) (Flynn and Flynn, 1998; Geider et al., 1998; Baumert and Petzoldt, 2008; Ross and Geider, 2009). For instance, Geider et al. (1998) proposed a phytoplankton growth formulation calibrated for chemostat experiments, in which chlorophyll production is proportional to both nitrogen assimilation and carbon fixation.

The different behaviours associated to these different growth formulations have generally been examined in the context of laboratory experiments

57 (Vatcheva et al., 2006), i.e. for monospecific cultures under a limited set  
58 of idealized forcing. Significant variations from Redfield stoichiometry ob-  
59 served in experimental data of nutrient-limited phytoplankton cultures have  
60 highlighted the limits of the Redfield-Monod-type models and the need for  
61 non-Redfieldian formulations (quota formulations) (Sciandra, 1991; Dearman  
62 et al., 2003; Flynn, 2003a, 2010). Besides, formulations that assume con-  
63 stant Chl:C ratio fail to reproduce experimental data (Flynn et al., 2001)  
64 or *in situ* observations (Doney et al., 1996; Lévy et al., 1998; Spitz et al.,  
65 1998). However, it is not straightforward to find the right trade-off between a  
66 model which is too simple to reproduce the observed dynamics and a complex  
67 model with too many free parameters to tune against limited data (Flynn,  
68 2003b). Based on comparisons with laboratory experiments, Flynn (2003a)  
69 suggested that quota-type models with empirical Chl:C relationship "should  
70 be adequate for most oceanographic modeling scenarios", although it must  
71 be kept in mind that even if a model using simplified assumptions may fit to  
72 observed data, it may not be acceptable (Mitra et al., 2007; Flynn, 2010).

73 A rigorous comparison of the qualitative and quantitative behaviours of  
74 Redfield, quota-type, and mechanistic models in more realistic oceanic con-  
75 ditions remains an open question. Based on model results at the Bermuda  
76 Atlantic Time-series Study (BATS) site, Schartau et al. (2001) suggested  
77 that an optimized model (i.e., after data assimilation procedure) with Red-  
78 field stoichiometry may not be able to correctly simulate primary production  
79 in oligotrophic subtropical regions, but, in an optimized marine ecosystem  
80 model of the Northwestern Mediterranean Sea, Faugeras et al. (2003) could  
81 not decipher significant differences between Redfield and quota growth for-

82 mulations.

83 In this context, the present work aims at comparing, in a rigorous frame-  
84 work, the qualitative and quantitative behaviours of different formulations of  
85 phytoplankton growth in an oceanographic context and to determine whether  
86 increasing complexity leads to significant improvement of the seasonal dy-  
87 namics of phytoplankton. This is examined with a 1D ecosystem model  
88 which simulates a seasonal cycle at BATS station. This site was chosen  
89 because strongly variable Chl:C and C:N ratios have been observed at this  
90 station over the year (for the phytoplankton and the particulate organic mat-  
91 ter, respectively; Sambrotto et al., 1993; Michaels and Knap, 1996; Steinberg  
92 et al., 2001). A coherent suite of consistent phytoplankton growth formula-  
93 tions is constructed by adding stepwise complexity. Constant, diagnostic,  
94 and prognostic Chl:C ratios are considered with Redfield stoichiometry or  
95 with variable C:N ratio. All formulations are then incorporated within the  
96 same ecosystem model applied in a 1D framework at BATS. Data assimila-  
97 tion through micro-genetic algorithm is used to calibrate the different models.  
98 This enables to compare the different formulations on the basis of their best  
99 performance relatively to standard observations.

100 After briefly presenting the study site, we describe the general structure of  
101 the marine ecosystem model and the different phytoplankton growth formu-  
102 lations. Then we present the micro-genetic algorithm used to tune the model  
103 parameters. In the Results section, the outputs of the different formulations  
104 are described and the skill of each formulation to reproduce observations  
105 is assessed. Finally, the choice of the phytoplankton growth formulation in  
106 marine biogeochemical models is discussed.

## 107 2. Models and methods

### 108 2.1. Study site

109 The Bermuda Atlantic Time-series Study (BATS) site is located in the  
110 Sargasso Sea, in the western North Atlantic subtropical gyre ( $31^{\circ}40'$  N,  
111  $64^{\circ}10'$  W). This station has been monthly sampled since October 1988 as  
112 part of the US Joint Global Ocean Flux Study (JGOFS) program and the  
113 data are freely available at <http://bats.bios.edu/index.html>. The sea-  
114 sonal dynamics of nitrate, chlorophyll and primary production at BATS have  
115 been described by Steinberg et al. (2001). In winter, strong vertical mixing  
116 supplies nutrients to the surface layers, allowing a moderate bloom to occur  
117 between January and March. In summer, nutrient supply collapses because  
118 of thermal stratification and primary production is low, with a subsurface  
119 chlorophyll maximum (60-120 m). *In situ* measurements also indicate that  
120 the stoichiometric ratios of particulate C, N and P deviate from the tradi-  
121 tional Redfield ratios, especially during the oligotrophic summer (Michaels  
122 and Knap, 1996; Cotner et al., 1997; Steinberg et al., 2001).

### 123 2.2. General model structure

124 The general structure of the model is a simple 'NPZD' type ecosystem,  
125 used in a 1D-framework which simulates the seasonal cycle of phytoplankton  
126 at BATS station. We used the LOBSTER marine ecosystem model, which  
127 has been previously used and calibrated for the North Atlantic (Lévy et al.,  
128 2005; Kremer et al., 2009; Lévy et al., 2012). Besides phytoplankton ( $P_N$ ),  
129 the ecosystem model has five additional prognostic variables expressed in ni-  
130 trogen units ( $\text{mmolN.m}^{-3}$ ): Nitrate ( $\text{NO}_3$ ), Ammonium ( $\text{NH}_4$ ), Zooplankton

131 ( $Z_N$ ), Detritus ( $D_N$ ), and Dissolved Organic Matter (DOM) (Fig. 1). The  
 132 photosynthetic available radiation (PAR) is derived from a two-wavelengths  
 133 light absorption model, with absorption coefficients depending on the lo-  
 134 cal phytoplankton concentrations. The detailed equations of the LOBSTER  
 135 model are presented in Table 1. The definition of the parameters and their  
 136 default values are presented in Table 2.

### 137 2.3. Model implementation

138 The ecosystem model is embedded in a simple 1D physical model, which  
 139 accounts for the observed seasonal evolution of the mixed layer depth (MLD)  
 140 and temperature at BATS in 1998. The 1D-model has 30 vertical layers,  
 141 with a vertical discretization of 10 m from 0-100 m and then increasing  
 142 with depth. Only vertical diffusion is taken into account. Monthly values  
 143 of observed MLD, temperature and salinity at BATS in 1998 are used and  
 144 linearly interpolated in time at each model time-step. The vertical eddy  
 145 diffusivities  $K_z$  are diagnosed from the MLD: they are set to  $1 \text{ m}^2.\text{s}^{-1}$  within  
 146 the mixed layer and to  $10^{-5} \text{ m}^2.\text{s}^{-1}$  below the mixed layer. A specific reaction  
 147 term  $sms$  (source minus sink) is added to the diffusion equation. For each of  
 148 the state variables  $i$ , the prognostic equation reads as follows:

$$\frac{\partial C_i}{\partial t} = \frac{\partial}{\partial z} \left( K_z \frac{\partial C_i}{\partial z} \right) + sms(C_i) \quad (1)$$

149 where  $C_i$  is the tracer concentration. The initial nitrate conditions are set  
 150 to *in situ* observations at BATS in January 1998, whereas they are set to  
 151  $0.1 \text{ mmolN.m}^{-3}$  for the dissolved organic matter, to  $0.03 \text{ mmolN.m}^{-3}$  for  
 152 the ammonium (Lipschultz, 2001), and to extremely low values for the other



153 state variables ( $10^{-8}$  mmolN.m<sup>-3</sup>). The biophysical model is spun up for one  
154 year and a time step of 1.2 hours is used.

#### 155 2.4. Increasing the complexity in the representation of phytoplankton

156 The complexity of phytoplankton growth formulations is progressively  
157 increased. Four levels of complexity are compared: 1) a Redfield formula-  
158 tion with constant Chl:C ratio, 2) a Redfield formulation with a diagnostic  
159 Chl:C ratio, 3) a quota formulation with a diagnostic Chl:C ratio, and 4) a  
160 quota formulation with a prognostic Chl:C ratio. In these formulations, the  
161 phytoplankton compartment is thus represented by 1, 2 or 3 state variables.  
162 For convenience, these formulations have then been named P1.0, P1.5, P2.5,  
163 and P3.0 respectively, with the arbitrary convention that a prognostic state  
164 variable counts for one and a diagnostic variable (chlorophyll) counts for a  
165 half.

##### 166 2.4.1. Redfield stoichiometry and constant Chl:C ratio (P1.0 formulation)

167 In the simplest formulation, phytoplankton are represented by a unique  
168 state variable (P1.0 formulation) (Fig. 2A, Tables 4 and 5). The phytoplank-  
169 ton carbon biomass  $P_C$  and nitrogen biomass  $P_N$  are related by a constant  
170 Redfield ratio  $R_{C:N} = P_C/P_N = 6.56$  molC.molN<sup>-1</sup>. The Chl:C ratio  $R_{Chl:C}$   
171 of the phytoplanktonic cells is also assumed to be constant and equal to  
172  $1/60$  gChl.gC<sup>-1</sup> (Fasham et al., 1990). Nitrogen uptake accounts for light  
173 and nutrient limitation. Light limitation  $L_I$  is defined according to Webb  
174 et al. (1974). Note that in order to keep the models as simple as possi-  
175 ble, this expression is shared by the four phytoplankton growth formulations  
176 P1.0, P1.5, P2.5, and P3.0. Nutrient-limitation  $L_N$  is expressed as the sum

177 of nitrate and ammonium limitations following Wroblewski (1977) and as  
178 used in Fasham et al. (1990). Primary production (in carbon currency) is  
179 proportional to nutrient uptake (in nitrogen currency) by the factor  $R_{C:N}$ .

#### 180 2.4.2. Redfield stoichiometry and diagnostic Chl:C ratio (P1.5 formulation)

181 The structure of the P1.5 formulation is similar to that of P1.0, except  
182 that photo-acclimation is accounted for (Tables 4 and 5). In this model, the  
183 phytoplanktonic chlorophyll:carbon ratio  $R_{Chl:C}$  is thus a diagnostic variable  
184 (Fig. 2B), calculated following Geider et al. (1996, 1998) as a function of  
185 light and nutrient limitation.

#### 186 2.4.3. Cell quota and diagnostic Chl:C ratio (P2.5 formulation)

187 In the P2.5 formulation, the phytoplanktonic nitrogen:carbon ratio  $Q =$   
188  $P_N/P_C$  is variable (quota formulation) (Tables 4 and 5). The phytoplanktonic  
189 compartment is thus represented by two state variables: the phytoplanktonic  
190 nitrogen biomass  $P_N$  and the phytoplanktonic carbon biomass  $P_C$  (Fig. 2C).  
191 As in P1.5, the phytoplanktonic chlorophyll:carbon ratio  $R_{Chl:C}$  is a diag-  
192 nostic variable calculated following Geider et al. (1998). The formulations of  
193 nutrient uptake and primary production have also been chosen following Gei-  
194 der et al. (1996, 1998). Nutrient uptake (in nitrogen currency) is expressed  
195 as the product of quota and nutrient limitation terms. Primary production  
196 (in carbon currency) is expressed as the product of quota and light limitation  
197 terms.

#### 198 2.4.4. Cell quota and prognostic chlorophyll (P3.0 formulation)

199 The P3.0 formulation corresponds to P2.5 with the addition of a fully  
200 prognostic equation for chlorophyll (Tables 4 and 5). Phytoplankton are thus

201 represented by three state variables: phytoplanktonic nitrogen biomass  $P_N$ ,  
 202 phytoplanktonic carbon biomass  $P_C$ , and chlorophyll biomass  $P_{Chl}$  (Fig. 2D).  
 203 The dynamical equation of the phytoplanktonic chlorophyll  $P_{Chl}$  is defined  
 204 following Geider et al. (1998): the chlorophyll production is a function of ni-  
 205 trogen uptake, carbon fixation (production) and light and it does not respond  
 206 rapidly to environmental changes when using the original set of parameters.

#### 207 2.4.5. Geider model (GP3.0 formulation)

208 All previous formulations share the same expression of light limitation,  
 209 which is independent of nutrient limitation and internal C:N quota, an as-  
 210 sumption that can be discussed (Flynn, 2003b, 2008). To check the conse-  
 211 quences of this assumption, a fifth model is constructed from P3.0 by using  
 212 the following light limitation term, which now depends on the internal C:N  
 213 quota  $Q$ :

$$L_I(Q) = \left[ 1 - EXP \left( - \frac{\alpha \cdot R_{Chl:C} \cdot PAR}{\mu_m \cdot \frac{Q - Q_0}{Q_{max} - Q_0}} \right) \right] \quad (2)$$

214 This new formulation, named GP3.0, corresponds to the original phytoplank-  
 215 ton growth formulation proposed by Geider et al. (1996, 1998), and which  
 216 has been previously incorporated in various marine ecosystem models (e.g.,  
 217 Moore et al., 2002; Lefèvre et al., 2003).

#### 218 2.5. Parameter tuning using micro-genetic algorithm

219 Model parameters are tuned using a micro-genetic algorithm to best fit  
 220 the observed seasonal cycle at BATS. Genetic algorithms are stochastic meth-  
 221 ods in which a population of parameters evolves with mutation/selection pro-  
 222 cesses (evolutionary tuning approach). In the particular case of micro-genetic  
 223 algorithms, the size of the population is small and no mutation is considered

224 (Carroll, 1996). A micro-genetic algorithm with binary coding, elitism, tour-  
225 nament selection of the parents, and uniform cross-over was used (Carroll,  
226 1996; Schartau and Oschlies, 2003). At the beginning, a set (or population)  
227 of parameter vectors (individuals) is randomly generated within a predefined  
228 range (Table 7). Each parameter vector is coded as a binary string (chro-  
229 mosome). Then, at each generation, the misfit of each parameter vector  
230 (fitness of each individual) is estimated as the misfit (cost function) between  
231 the data and the model outputs for this parameter vector. The parameter  
232 vector with the lowest misfit (best individual of its generation or 'elite') is  
233 conserved to the next generation. Then, four vectors are randomly chosen  
234 and associated in two pairs. The vectors with the lowest misfit (best fitness)  
235 within each pair are selected (parents), and a new parameter vector (child)  
236 is produced by randomly crossing each bit of the two selected vectors. This  
237 process (reproduction) is repeated until the replenishment of the population.  
238 New generations are produced (evolution), until the population of parameter  
239 vectors has converged (all the vectors are identical to the elite). Then, a  
240 new generation is randomly generated, with the elite conserved. This pro-  
241 cess was repeated 500 times for a population whose size was chosen equal  
242 to the number of parameters to identify (Schartau and Oschlies, 2003). For  
243 each model, the parameter space was reduced to the parameters for which  
244 the cost function was the most sensible, as learnt from preliminary sensibility  
245 analyses (four to six parameters depending on the model, see Table 7).

#### 246 2.6. Cost function and model comparison

247 *In situ* data measured at BATS in 1998, including monthly records of ni-  
248 trate concentration, total particulate organic nitrogen concentration, chloro-

249 phyll concentration, and primary production, are used for optimization. In  
 250 the model, total particulate organic nitrogen (PON) is taken as the sum  
 251 of phytoplanktonic nitrogen, zooplanktonic nitrogen and detritus:  $PON =$   
 252  $P_N + Z_N + D_N$ . These monthly profiles are re-gridded along the 1D ver-  
 253 tical grid of the model. The cost function  $F$  is taken as the weighted  
 254 sum of squared differences between monthly vertical profiles of observations  
 255  $obs_n(k, l)$  and model outputs  $mod_n(k, l)$  (Evans, 2003; Stow et al., 2009):

$$F = \frac{1}{KL} \sum_{n=1}^N \sum_{k=1}^K \sum_{l=1}^L W_n [obs_n(k, l) - mod_n(k, l)]^2 \quad (3)$$

256 Four data types are used ( $N = 4$ ): nitrate concentration, chlorophyll concen-  
 257 tration, total particulate organic nitrogen and primary production. The cost  
 258 function is calculated from monthly data ( $L=12$ ) and only the first vertical  
 259 layers from 0 to 168 m are used ( $K=15$ ). The weights  $W_n$  are chosen equal  
 260 to the inverse of the standard deviation of the monthly observations ( $1/\sigma_n$ ),  
 261 with  $\sigma_{NO_3} = 0.541 \text{ mmolN.m}^{-3}$ ,  $\sigma_{Chl} = 0.080 \text{ mgChl.m}^{-3}$ ,  $\sigma_{PON} = 0.106$   
 262  $\text{mmolN.m}^{-3}$ ,  $\sigma_{PP} = 0.177 \text{ mmolC.m}^{-3}.\text{d}^{-1}$ .

263 Model outputs are also compared with *in situ* data and with each other  
 264 using skill assessment technics, such as Taylor diagrams and target diagrams  
 265 (Taylor, 2001; Stow et al., 2009; Jolliff et al., 2009). These diagrams can be  
 266 seen as complementary indicators of the misfit between data and model out-  
 267 puts, including correlation, root mean squared differences, relative standard  
 268 deviations, and bias.

### 269 3. Results

#### 270 3.1. Parameter tuning using micro-genetic algorithm

271 For each phytoplankton growth formulation, four to six parameters are  
272 identified through an optimization algorithm, with the number of optimized  
273 parameters increasing with the formulation complexity. The parameter val-  
274 ues obtained after optimization are in the same range of magnitude among  
275 the different models (Table 8). We can note that, after optimization and  
276 compared to their initial default values, grazing parameters ( $K_{g,g}$ ) and max-  
277 imal Chl:N ratio ( $R_{Chl:N}^{Max}$ ) are increased, whereas the other parameters remain  
278 close to their default values. For each model, the best constrained parameter  
279 is the initial PI slope  $\alpha$  (as indicated by the evolution of the minimum mis-  
280 fit obtained for each of the 64 possible values of this parameter during the  
281 optimization procedure, not shown).

282 After optimization, cost functions are reduced for all models, by 23% for  
283 P1.0 to 38% for P2.5 (Table 8). Model performances to reproduce all data  
284 types are improved (Fig. 3). The optimizations increase the correlation be-  
285 tween the model outputs and the observations (angular coordinates on the  
286 Taylor diagram) and decrease the ratio of the standard deviations of model  
287 outputs and observations (radial coordinates on the Taylor diagram). Op-  
288 timizations also decrease the bias and the normalized unbiased root mean  
289 squared differences between model outputs and observations (abscissae and  
290 ordinates on the Target digram). Nitrate is the observation which is glob-  
291 ally best reproduced by all models, contrary to particulate organic nitrogen  
292 (PON).

293 *3.2. Seasonal dynamics*

294 The temporal evolution of the vertical profiles of nitrate, PON, chloro-  
295 phyll and primary production confirms that all the models, after the param-  
296 eter identification procedure, behave similarly. This may suggest a strong  
297 impact of the initial conditions and physical forcing (Fig. 4). The evolutions  
298 of nitrate and PON distributions are not significantly different between the  
299 phytoplankton growth formulations. In response to the deepening of the  
300 mixed layer in March, nitrate is entrained to the surface. It is then quickly  
301 consumed in the euphotic layer during winter and spring, leaving very low ni-  
302 trate concentrations in summer. Accordingly, PON and chlorophyll exhibit a  
303 strong seasonal variability with a strong contrast between winter/spring and  
304 summer. A strong phytoplankton bloom occurs between March and April,  
305 characterized by high PON and chlorophyll concentrations in the surface  
306 mixed layer, followed by a subsurface maxima in chlorophyll in summer.

307 Larger differences between phytoplankton growth formulations can be  
308 seen in chlorophyll and production, with larger discrepancies between simu-  
309 lations and observations than among simulations (Fig. 4). None of the model  
310 correctly reproduces the exact dynamics of the observations. All models  
311 are able to reproduce the subsurface chlorophyll maximum in summer, but  
312 simulated chlorophyll concentrations are lower than observed whatever the  
313 model, except during the bloom. None of the models is able to reproduce  
314 the observed temporal evolution of production, which is characterized by a  
315 maximum value in February and high values during the oligotrophic sea-  
316 son. However, the high production period is longer for quota formulations.  
317 As expected from previous studies (Doney et al., 1996; Spitz et al., 1998),

318 the Redfield formulation with constant Chl:C ratio (P1.0) is unable to si-  
319 multaneously reproduce the deep chlorophyll maximum and the subsurface  
320 production maximum during the oligotrophic season, because of its constant  
321 Chl:C ratio (Fig. 5). Conversely, models with photo-acclimation (i.e., vari-  
322 able Chl:C ratio) are all able to simulate the deep chlorophyll maximum and  
323 the subsurface production maximum during the oligotrophic season. Taking  
324 into account photo-acclimation allows to increase the C:Chl ratio in surface,  
325 especially during oligotrophic conditions (Fig. 5).

326 The cell quota formulations with photo-acclimation (P2.5, P3.0 and GP3.0)  
327 exhibit significant differences from the Redfield formulations in terms of  
328 C:Chl ratio, phytoplankton biomass in carbon, and C:N ratio, particularly  
329 during oligotrophic conditions (Fig. 5). During the bloom, lower C:Chl and  
330 C:N ratios are simulated by the models that allow these ratios to vary. Dur-  
331 ing the oligotrophic period, higher C:Chl and C:N ratios are simulated at the  
332 surface by these models, with very close values for the three formulations.  
333 The Redfield formulation with photo-acclimation (P1.5) simulates the lowest  
334 variations of the C:Chl ratio, suggesting that this model could be less efficient  
335 than the quota formulations to simulate photo-acclimation, likely because it  
336 is less flexible.

### 337 *3.3. Annual and seasonal production in carbon and nitrogen*

338 In general, similar total and new productions in nitrogen are simulated  
339 by the different models (relative differences about 5 %), except for the new  
340 production between P1.0 and P2.5 (about 30 % higher for P2.5) (Table 9).  
341 F-ratios vary from 0.43 to 0.49 during the bloom and from 0.20 to 0.27 dur-  
342 ing the oligotrophic period. Total productions in carbon are much larger



343 for the formulations with a variable C:N quota than for the Redfield for-  
344 mulations (about 50 % larger). This increase in carbon production is simu-  
345 lated both during the bloom and during oligotrophic conditions, suggesting a  
346 more efficient photosynthesis per chlorophyll content. Temporal evolution of  
347 vertically-integrated daily production in nitrogen are close between models,  
348 whereas strong differences are observed in vertically-integrated daily produc-  
349 tion in carbon between Redfield and quota formulations, both during the  
350 bloom and in summer (Fig. 6).

351 With cell quota formulations (P2.5, P3.0 and GP3.0), the C:N ratio of  
352 total production is higher than the Redfield ratio and it increases at the  
353 surface in summer, i.e. during oligotrophic conditions, with the highest C:N  
354 values simulated by GP3.0 (about 15 at the surface at the end of the year)  
355 (Fig. 7). Note that this feature is an emergent property of these cell quota  
356 formulations, since the value of the C:N ratio was not constrained during  
357 the optimization procedure. Besides, with the cell quota formulations the  
358 C:N ratio of total production is always higher than the C:N ratio of phyto-  
359 plankton, because of the cost of the nitrogen uptake ( $\zeta$  parameter). With  
360 the P2.5 formulation, for instance, the C:N ratios of total production and  
361 of phytoplankton vary between 9 and 14  $molC.molN^{-1}$  and between 5 and  
362 10  $molC.molN^{-1}$ , respectively.

#### 363 4. Discussion

364 The aim of the present work was to assess the consequences of taking into  
365 account photo-acclimation and variable stoichiometry of the phytoplankton  
366 growth in marine ecosystem models, by comparing the qualitative and quan-

367 titative behaviours of several growth formulations within a rigorous frame-  
368 work. A parameter tuning based on optimization procedure was performed  
369 before the comparison, using observed data of nitrate, particulate organic  
370 nitrogen (PON), chlorophyll, and primary production at BATS. The opti-  
371 mization increases the ability of all models to reproduce the observed data.  
372 Globally, all models behave similarly after optimization and no difference  
373 in the ability to reproduce nitrate or PON data is observed. However, as  
374 expected from previous studies at BATS (Doney et al., 1996; Spitz et al.,  
375 1998), photo-acclimation (i.e., a variable Chl:C ratio) is needed to simul-  
376 taneously reproduce subsurface production and deep chlorophyll maximum  
377 during oligotrophic conditions in summer. Moreover, Redfield formulations  
378 underestimated production compared to quota formulations, which suggests  
379 that the latter should be preferred. No clear difference is detected between  
380 quota formulations with diagnostic or prognostic chlorophyll. Our main con-  
381 clusion is that quota formulations with diagnostic or prognostic chlorophyll  
382 enable to simulate more realistic values of chlorophyll and phytoplankton  
383 production during oligotrophic conditions, compared with formulations with  
384 constant Chl:C and C:N ratios. Indeed, these formulations are able to simu-  
385 late a more 'flexible' phytoplankton physiology. They are then able to better  
386 reproduce the phytoplankton dynamics under a wider range of environmental  
387 conditions.

#### 388 *4.1. Parameter tuning*

389 In order to compare the different phytoplankton growth formulations, we  
390 have followed the methodology which consists in calibrating parameters prior  
391 to comparison using advanced parameter estimation approaches (Faugeras

392 et al., 2004; Friedrichs et al., 2006; Smith and Yamanaka, 2007; Ward et al.,  
393 2010; Bagniewski et al., 2011). This ensures that all models performed the  
394 best they could. Sensitivity analyses have been needed to properly choose  
395 the cost function and the parameters to calibrate with the optimization pro-  
396 cedure: the sensitivity of several cost functions have been tested *a priori*  
397 and only the most constrained parameters have been selected as candidates  
398 for the minimization algorithm. Optimization procedure also provides *a pos-*  
399 *teriori* estimates of the parameter uncertainty (Matear, 1995; Fennel et al.,  
400 2001; Faugeras et al., 2003; Schartau and Oschlies, 2003). For instance, using  
401 dissolved inorganic nitrogen, PON, chlorophyll, silicate, and oxygen data to  
402 optimize the parameters of a simple marine ecosystem model through varia-  
403 tional optimization, Bagniewski et al. (2011) concluded that phytoplankton  
404 parameters (such as  $\mu$ ,  $\alpha$ , and  $m_P$ ) were better constrained than zooplankton  
405 parameters (such as  $g$ ). In the present study, the strength of the minimiza-  
406 tion algorithm has been qualitatively estimated from the shape of the misfit  
407 function for each of the selected parameters. The best constrained parameter  
408 is the initial PI slope  $\alpha$ , which is not surprising since this parameter appears  
409 in the equations of nitrate, PON, chlorophyll, and primary production, i.e.,  
410 the data used during the optimization procedure.

#### 411 4.2. Model framework

412 For the purpose of our study, we used a relatively simple biogeochemi-  
413 cal model and the annual primary production in carbon was underestimated  
414 with all the phytoplankton growth formulations (assuming the production  
415 data are correct). This shortcoming is a problem faced by most biogeochem-  
416 ical models in the North Atlantic subtropical gyre (see for instance Oschlies,

417 2002). Several reasons can be advanced to explain it. One reason is the  
418 use of a simple 1D physical framework, since lateral transport, which could  
419 provide an additional source of DOM that would then be remineralized *in*  
420 *situ* (Williams and Follows, 1998), and nutrient supply by mesoscale and sub-  
421 mesoscale processes (Oschlies, 2002; McGillicuddy et al., 2003; Lévy et al.,  
422 2012) may significantly increase the production in the North Atlantic. A  
423 second hypothesis is the lack of nitrogen-fixers in our model. Finally, a third  
424 hypothesis would be that the structure of the model is not complex enough,  
425 in particular because of the lack of explicit bacteria. Indeed, this compart-  
426 ment may play an important role during summer, especially for regenerated  
427 production (Steinberg et al., 2001). However, the presence of a DOM pool in  
428 our model implicitly assumes remineralization through bacterial activity and  
429 allows local remineralization of the organic matter being produced. Besides,  
430 the LOBSTER model have been complexified with an explicit representa-  
431 tion of bacteria and the versions of LOBSTER with and without bacteria  
432 have been compared in the Mediterranean sea and showed little differences  
433 in terms of primary production, even during the summer oligotrophic period  
434 (Lévy et al., 1998). Moreover, sensitivities to the DOM remineralization rate,  
435 which mimics the action of bacteria, did not enable to significantly change  
436 the simulated primary production, further highlighting that the reason for  
437 this might more probably be the lack of nitrogen sources in the model rather  
438 than to the simplified microbial network. This model could also have been  
439 improved by the representation of additional phytoplankton types, since the  
440 composition of the phytoplankton community changes along the year, or  
441 by the use of additional nutrients such as phosphate (Cotner et al., 1997;

442 Steinberg et al., 2001), but then it would have required to take into account  
443 multi-nutrient growth limitation of phytoplankton. Although a better agree-  
444 ment between model and observation might then be obtained using a more  
445 complex biogeochemical model and/or a more realistic physical forcing, the  
446 model framework can be used to compare the different phytoplankton growth  
447 formulations in a robust manner.

#### 448 *4.3. Photo-acclimation in marine biogeochemical models*

449 Our comparative modelling study at BATS suggests that taking into ac-  
450 count photo-acclimation (i.e., a variable Chl:C ratio) is mandatory to si-  
451 multaneously reproduce deep chlorophyll maximum and subsurface primary  
452 production during oligotrophic conditions. Indeed, a model without photo-  
453 acclimation (P1.0) is able to predict the spring bloom and the depth of the  
454 chlorophyll maximum, but has difficulties to reproduce the high production  
455 observed in summer in subsurface, compared to the formulations with photo-  
456 acclimation that are more flexible. Since in the latter formulations the Chl:C  
457 ratio can vary depending on environmental conditions (namely light and nu-  
458 trient availability), they can better perform along a wider range of conditions  
459 (surface and subsurface, spring and summer).

460 These results are in agreement with previous modelling studies at BATS  
461 indicating that the phytoplankton dynamic could not be reproduced when  
462 using a constant Chl:C ratio (Doney et al., 1996; Hurtt and Armstrong, 1996,  
463 1999; Spitz et al., 1998, 2001; Fennel et al., 2001). Doney et al. (1996) hy-  
464 pothesized that this may be "because not enough nutrient were available  
465 to sustain [the production in summer]". Our comparative study highlights  
466 that difficulties to simulate the high production in summer may partly be

467 due to the fixed Chl:C ratio, since models with variable Chl:C were able to  
468 reproduce the observations better. Similarly, Fennel et al. (2001) and Spitz  
469 et al. (1998) could not correctly reproduce observation data at BATS with  
470 simple NPZD models with constant Redfield and Chl:N ratios, even after  
471 parameter optimization. Fennel et al. (2001) suggested that this was due  
472 to the physical forcing and/or to the too simple hypotheses of the ecosys-  
473 tem model, whereas Spitz et al. (1998) proposed three possible explanations  
474 for this failure: the use of a Redfield stoichiometry, the absence of photo-  
475 acclimation, and approximations about vertical processes. In the present  
476 study, the same physical forcing is used for all models and our results indi-  
477 cate that the failure to reproduce the nitrate and chlorophyll data may be  
478 due to the absence of photo-acclimation (constant Chl:N ratio). Our results  
479 are in agreement with the improvements of the Fasham model proposed by  
480 Hurtt and Armstrong (1996, 1999) using a variable Chl:N ratio as a function  
481 of the irradiance, or by Spitz et al. (2001) using a prognostic Chl:N ratio:  
482 photo-acclimation of phytoplankton should be taken into account to simulate  
483 the subsurface chlorophyll maximum under summer oligotrophic conditions.  
484 In summer this chlorophyll maximum is observed in subsurface, with max-  
485 imum production rates at the surface. This means that the phytoplankton  
486 decrease its pigment content at the surface and increase it to collect more  
487 light in subsurface. Our results suggest that such flexibility in phytoplankton  
488 physiology can only be simulated in marine ecosystem models if the ratio of  
489 pigment content over biomass can vary depending on environmental condi-  
490 tions (photo-acclimation).

491 Our suite of numerical experiments also allows to compare several formu-

492 lations of photo-acclimation. The P2.5 formulation, with diagnostic chloro-  
493 phyll, and the P3.0 formulation, with fully dynamical chlorophyll, produced  
494 relatively similar results. Slight differences were observed between the P3.0  
495 and the GP3.0 formulations, both with dynamical chlorophyll but with differ-  
496 ent light limitation formulations. In the latter, light limitation is a function  
497 of the cell quota, as recommended by Flynn (2003b) to assure that, at steady  
498 state, the growth-irradiance curve has the correct initial slope. However, phy-  
499 toplankton growth in the ocean is often not at steady state. Additional data  
500 on phytoplanktonic carbon concentration and C:N ratio would be needed  
501 to constrain these cell quota formulations with photo-acclimation and com-  
502 pare their ability to reproduce phytoplanktonic dynamics. In the meantime,  
503 and as suggested by Flynn (2003a) from growth formulation comparison for  
504 laboratory experiments, phytoplankton models with diagnostic chlorophyll  
505 should be preferred when coupled with marine ecosystem models.

#### 506 *4.4. Stoichiometry of phytoplanktonic production*

507 Our results indicate that compared to Redfield growth formulations, quota  
508 growth formulations better reproduce the primary production during oligo-  
509 trophic conditions. Several problems arose from previous modelling studies  
510 at BATS using constant C:N ratios with photo-acclimation because of the  
511 assumed Redfield stoichiometry. Schartau et al. (2001) concluded that pro-  
512 duction data could not be reproduced after optimization when a constant  
513 C:N ratio was assumed. Schartau and Oschlies (2003) also indicated that the  
514 parameter optimization of a Redfield NPZD model with photo-acclimation  
515 leads to high value of the parameter  $\alpha$  (initial PI slope) "likely [to] com-  
516 pensat[e] for a deficiency in the parameterization of light-limited growth."

517 Finally, Oschlies and Schartau (2005) concluded that their model was unable  
518 to reproduce the observed data after optimization due "both to errors in  
519 the physical model component and to errors in the structure of the ecosys-  
520 tem model, which an objective estimation of ecosystem model parameters by  
521 data assimilation alone cannot resolve." Besides, the stoichiometry of total  
522 particulate organic matter is known to be non-Redfield at BATS (Michaels  
523 and Knap, 1996; Cotner et al., 1997), as already reported in other parts of  
524 the North Atlantic (Sambrotto et al., 1993; Kortzinger et al., 2001). Sur-  
525 face and mixed layer values of the C:N ratio of particulate organic matter  
526 recorded at BATS in 1998 vary from 6.19 to 10.26  $molC.molN^{-1}$ , with val-  
527 ues larger than 8  $molC.molN^{-1}$  from June to August (Fig. 7). However,  
528 the comparison of these observed values with simulated C:N ratios of pro-  
529 duction and phytoplankton are not straightforward, since the proportions  
530 of phytoplanktonic nitrogen and carbon relative to total particulate organic  
531 nitrogen and carbon are unknown. Nevertheless, the increase of C:N ratios  
532 during oligotrophic conditions is well reproduced by the cell quota formula-  
533 tions, because of low nutrient availability during the summer. For cell-quota  
534 formulations, it is then the ability of the C:N ratio to vary under changing  
535 environmental conditions (flexibility) that is responsible to a more realistic  
536 simulated production.

537 Similarly, an *in situ* study of the evolution of the C:N ratios of particu-  
538 late organic matter and production in the mixed layer in the North-East At-  
539 lantic indicated that these C:N ratios were higher during summer than during  
540 spring, with values of C:N ratio of production of 10-16 and 5-6  $molC.molN^{-1}$ ,  
541 respectively (Kortzinger et al., 2001). These results suggest that our conclu-



542 sions at BATS may extend to other areas in the ocean. Besides, it would be  
543 interesting to adapt this study to a station where data of phytoplanktonic  
544 nitrogen and carbon would be available in order to discriminate between the  
545 different quota formulations (P2.5, P3.0, and GP3.0).

#### 546 *4.5. Implications for marine ecosystem modelling*

547 Several recent studies, that have compared different biogeochemical mod-  
548 els, have focused on the structure of the model rather than on the formu-  
549 lation of phytoplankton growth (Friedrichs et al., 2006, 2007; Ward et al.,  
550 2010; Kriest et al., 2010; Bagniewski et al., 2011). Friedrichs et al. (2006)  
551 found that a change in the physical model had a more important impact than  
552 a change in the ecosystem model complexity. Similarly, Kriest et al. (2010)  
553 demonstrated that increasing complexity of a simple biogeochemical model at  
554 global scale did not necessarily improve the model's performance. Neverthe-  
555 less, the choice of model complexity (food web structure, description of key  
556 physiological processes, parameter estimations, plankton functional types) is  
557 one of the challenges of future marine ecosystem modelling (Flynn, 2003a;  
558 Le Quéré et al., 2005; Flynn, 2010; Anderson, 2010; Allen and Fulton, 2010;  
559 Allen and Polimene, 2011). Besides, the use of complex models is still under  
560 debate because of our lack of specific knowledge in parameterizing plankton  
561 physiology and its variability (Anderson, 2005; Allen et al., 2010; Allen and  
562 Polimene, 2011).

563 Our study allows to quantify the error made when a constant Redfield  
564 stoichiometry is considered (instead of a variable C:N ratio) in phytoplank-  
565 ton growth formulation, as it is still the case in most biogeochemical mod-  
566 els, especially when they are used at global scale. Indeed, only a few global

567 ecosystem models decouple nitrogen and carbon dynamics (Vichi et al., 2007;  
568 Vichi and Masina, 2009). A recent study using a marine ecosystem model at  
569 global scale decoupled nitrogen and phosphorus dynamics relative to carbon,  
570 but still used a Monod-type version of nutrient limitation (Tagliabue et al.,  
571 2011). This model was thus "in between" Monod-Redfield and cell quota for-  
572 mulations. Global scale models that decouple carbon and nitrogen uptakes  
573 are particularly needed to study the impact of increased CO<sub>2</sub> in the ocean.  
574 Indeed, carbon dioxide enhances carbon fixation but not dissolved inorganic  
575 nitrogen uptake, thus potentially increasing C:N ratios. Such processes have  
576 already been observed in mesocosm experiments (Riebesell et al., 2007), and  
577 should now be incorporated in global marine ecosystem models. Besides, cli-  
578 mate change will likely modify to some degree the stoichiometry of inorganic  
579 and organic C:N:P in the oceans (Hutchins et al., 2009). For these reasons,  
580 models without enough 'flexibility' in their formulation will not be able to  
581 represent the non-linearities between carbon and nitrogen assimilation. In  
582 parallel with model improvements, field and *in situ* experiments should con-  
583 tinue in collaboration with modelers to increase our knowledge in plankton  
584 physiology and dynamics under varying environment and provide data to  
585 calibrate and validate models.

## 586 **5. Conclusion**

587 The aim of the present work was to assess the advantages of taking into  
588 account photo-acclimation and variable stoichiometry of the phytoplankton  
589 growth in marine ecosystem models. After parameter calibration through  
590 an optimization procedure, lower misfits with observed data at BATS were

591 simulated when photo-acclimation and non-Redfield stoichiometry were con-  
592 sidered (i.e., variable Chl:C and C:N ratios). The main differences in qual-  
593 itative and quantitative behaviours of phytoplankton growth models were  
594 observed under oligotrophic conditions, because of the lack of model flexibil-  
595 ity. In agreement with previous studies, photo-acclimation was mandatory  
596 to simultaneously reproduce the observed deep chlorophyll maximum and  
597 subsurface production during oligotrophic conditions. Moreover, quota for-  
598 mulations enabled a better agreement with production data in subsurface and  
599 during oligotrophic conditions than Redfield formulations. No clear differ-  
600 ence was detected between quota formulations with diagnostic or prognostic  
601 chlorophyll, and more data would be needed to discriminate between these  
602 quota formulations with photo-acclimation. Future work would embed these  
603 different phytoplankton growth formulations within a 3D physical model to  
604 test whether our results can be generalized under contrasted oceanic regime  
605 and at basin scale (Ayata et al., *in prep.*).

## 606 **6. Acknowledgements**

607 This work was supported by the *Action Collaborative de Recherche* NAU-  
608 TILUS funded by the french *Institut National de la Recherche en Informa-*  
609 *tique et en Automatismes* (INRIA) and is part of the TANGGO initiative  
610 supported by the CNRS-INSU-LEFE program. SDA was supported by a  
611 post-doctoral fellowship from INRIA. The authors would like to thank Kevin  
612 Flynn and an anonymous reviewer for their constructive comments on a first  
613 version of this manuscript.

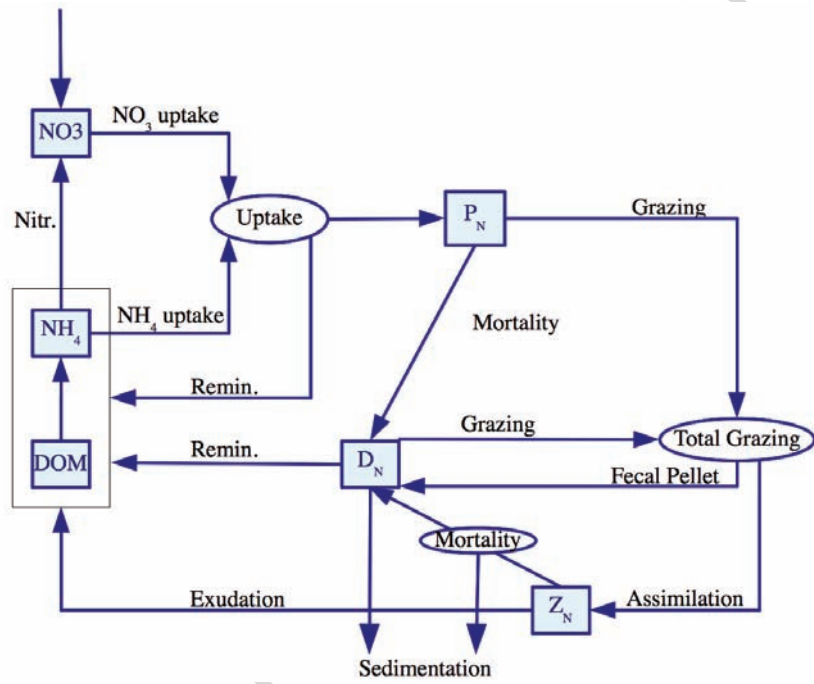


Figure 1: Structure of the LOBSTER marine ecosystem model. The six state variables are in nitrogen currency (blue color). The detailed equations of the model are given in Table 1. Nitr.: Nitrification; Remin.: Remineralization.

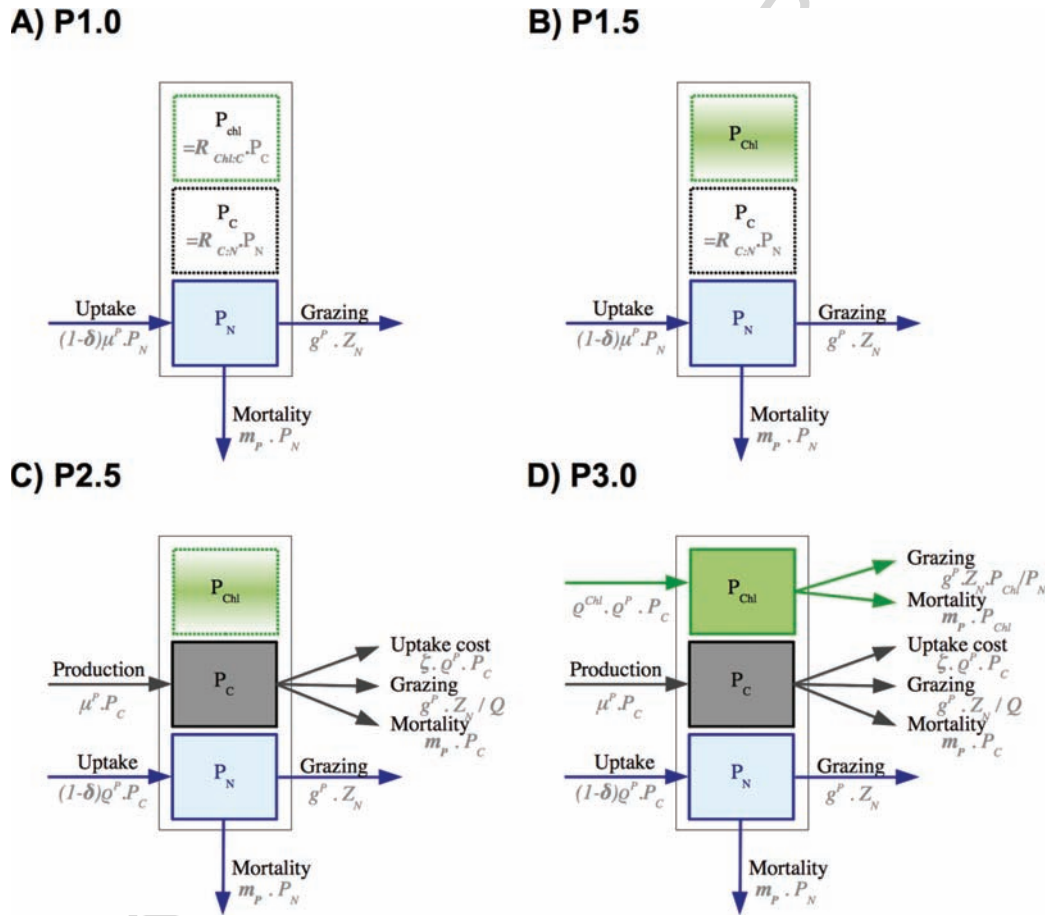


Figure 2: Structure of the phytoplankton growth formulations: A) Redfield formulation with constant chlorophyll:carbon ratio (P1.0), B) Redfield formulation with diagnostic chlorophyll (P1.5), C) quota formulation with diagnostic chlorophyll (P2.5), and D) quota formulation with prognostic chlorophyll (P3.0). Note that the Geider formulation (GP3.0) shares the same structure as P3.0. State variables are in plain color and diagnostic variables in shaded color. The colors of the variables indicate their currency: blue for nitrogen, grey for carbon, and green for chlorophyll.

Figure 3: Taylor and target diagrams of the monthly vertical profiles of nitrate concentration (diamonds), PON concentration (triangles), chlorophyll concentration (circle) and primary production (square) calculated for each formulation with default parameters (empty symbol) and after optimization (full symbol). The Taylor diagram represents in polar coordinates the normalized standard deviation and the correlation between observation and model output. On this diagram, the distance with the point of coordinates (1,0) measures the normalized root mean squared differences between observation and model output.

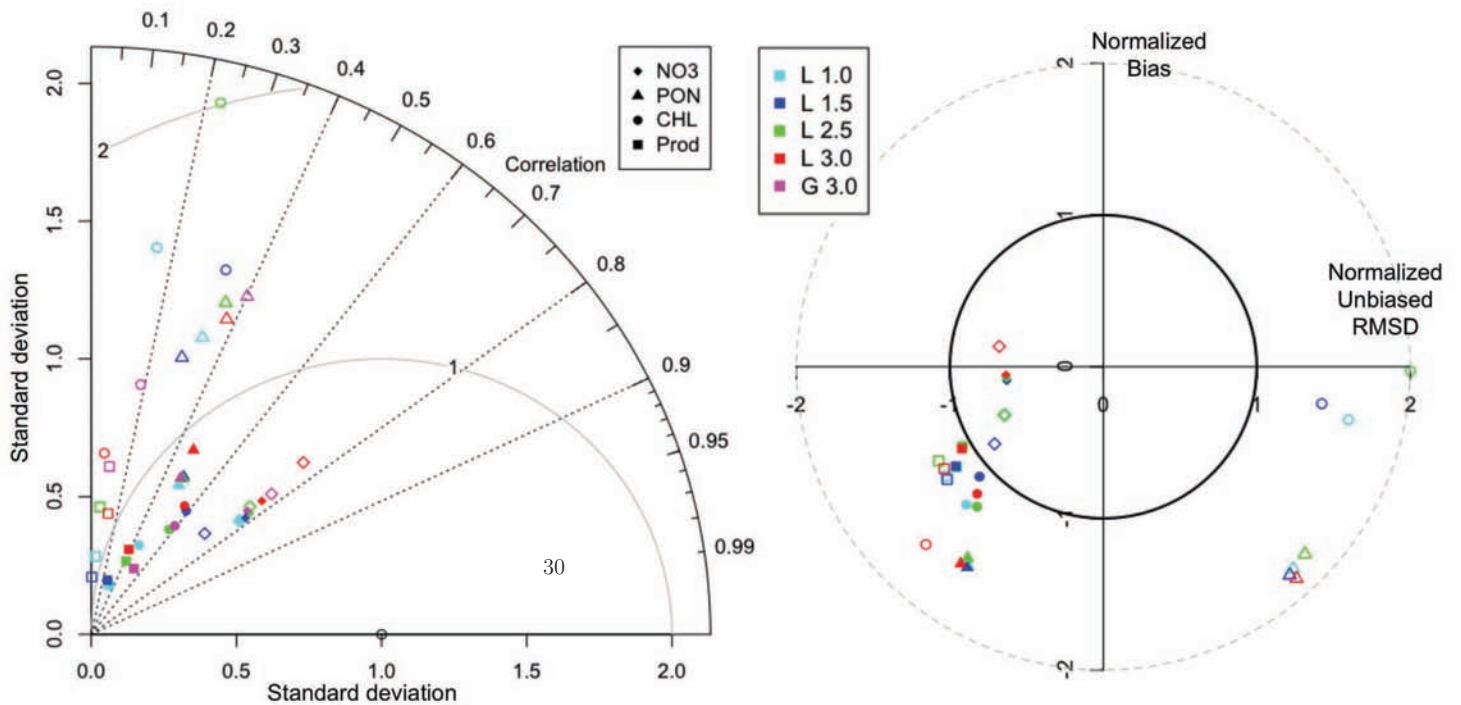


Figure 4: Seasonal cycles of nitrate, particulate organic nitrogen (PON), chlorophyll, and primary production at BATS in 1998, simulated with the different models after optimization and observed at BATS in 1998. The observed mixed layer depth is superimposed in white over the observed nitrate profiles.

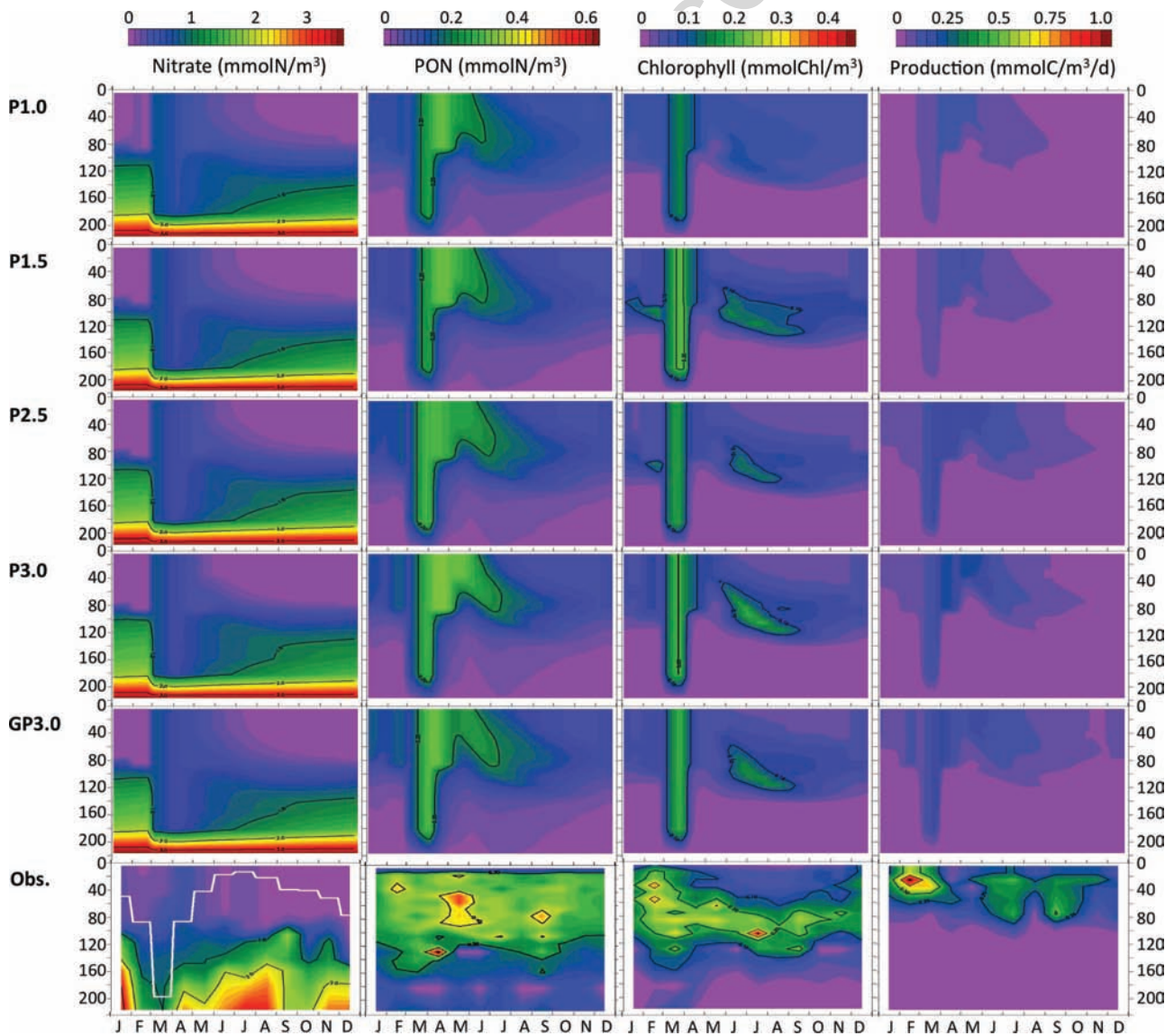


Figure 5: Average vertical profiles during boom (Mar-Apr) and during oligotrophic conditions (Jul-Aug) of the concentrations of phytoplanktonic nitrogen, phytoplanktonic carbon, C/ N ratio and C:Chl ratio, simulated with P1.0 (dark blue), P1.5 (light blue), P2.5 (green), P3.0 (red), and GP3.0 (magenta) after optimization.

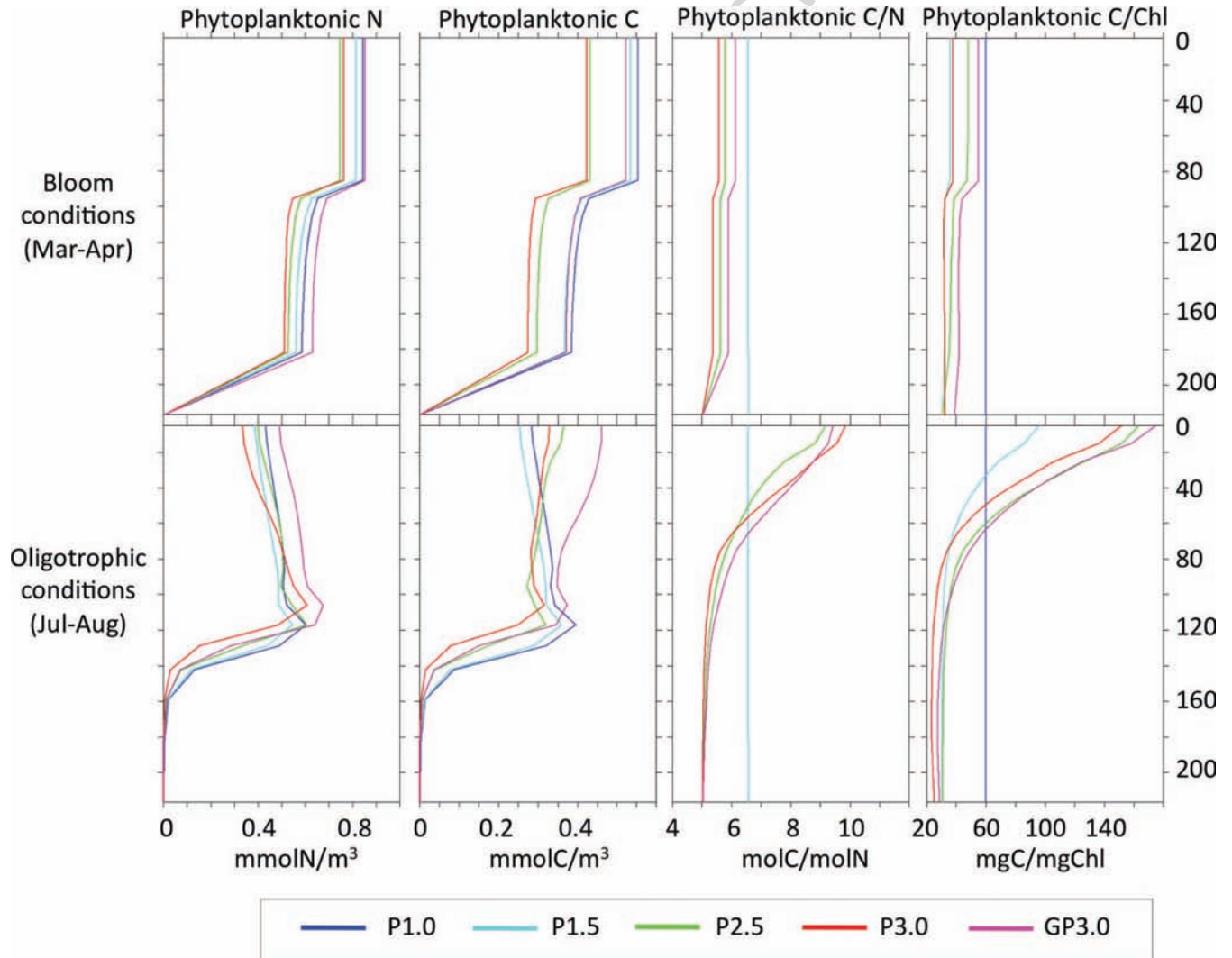




Figure 6: Temporal evolution of integrated daily production in carbon and in nitrogen from 0 to 234 m, simulated by the Redfield formulations P1.0 (blue) and P1.5 (light blue), and by the quota formulations P2.5 (green), P3.0 (red), and GP3.0 (magenta) after optimization. The observed values of the integrated daily production in carbon at BATS are indicated (black crosses).

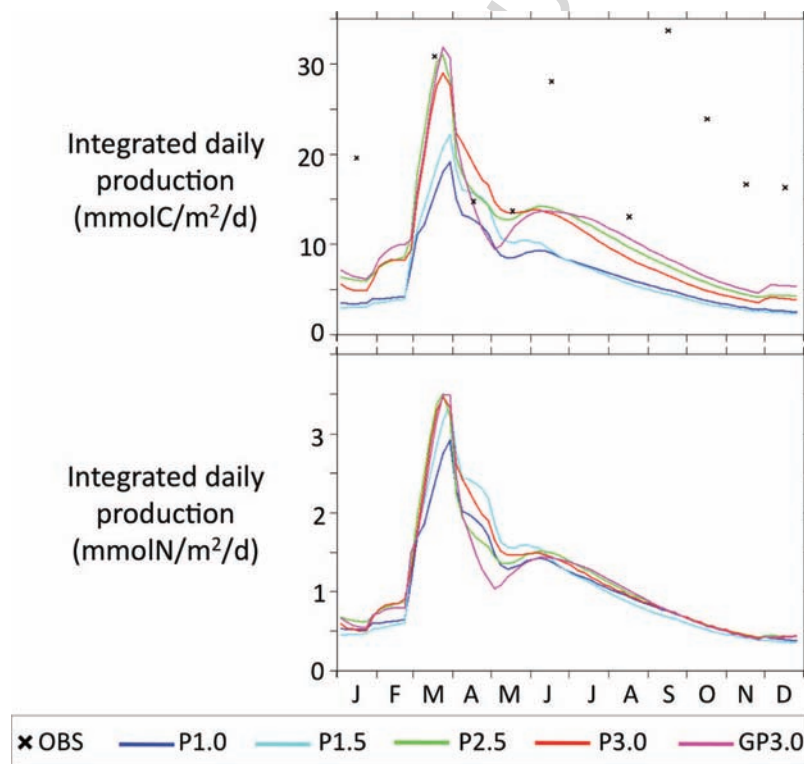


Figure 7: Temporal evolution of the C:N ratio of the production and of the phytoplankton at 0-10 m, 40-50 m and 90-100 m after optimization, simulated by the Redfield formulations P1.0 and P1.5 (light blue), and by the quota formulations P2.5 (green), P3.0 (red), and GP3.0 (magenta). The C:N ratio of the production is calculated as the ratio between the total production in carbon and the total production in nitrogen. The observed surface values of the C:N ratio of the total particulate organic matter measured at BATS in 1998 are superimposed on the simulated C:N ratio of the phytoplankton (black crosses).

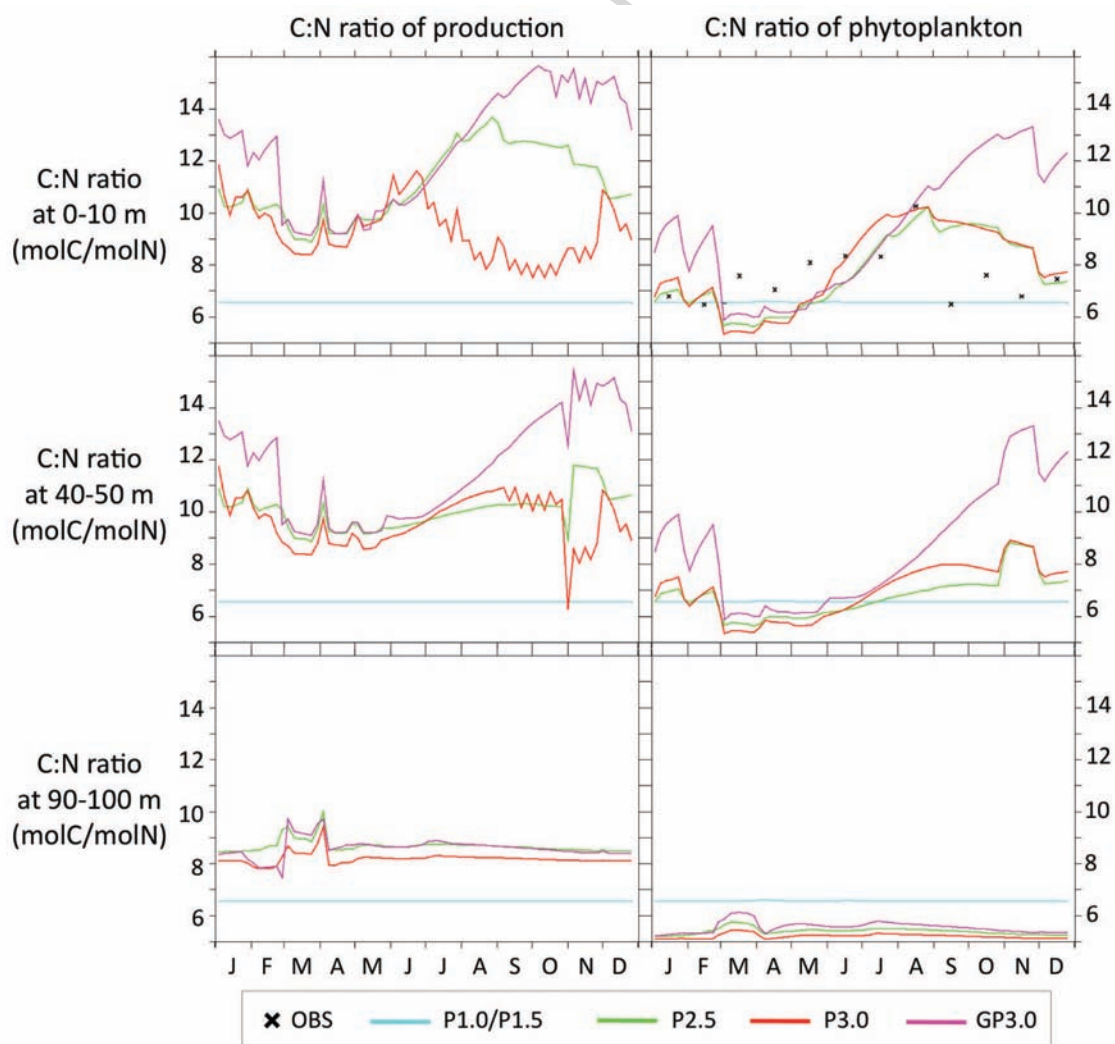


Table 1: Equations of the LOBSTER marine ecosystem model. The source minus sink (*sms*) terms of the equations are given for each of the six state variables of the model (in nitrogen currency): nitrate ( $\text{NO}_3$ ), ammonium ( $\text{NH}_4$ ), phytoplankton ( $P_N$ ), zooplankton ( $Z_N$ ), detritus ( $D_N$ ), and dissolved organic matter (DOM). The phytoplankton growth formulation is a Redfield formulation with constant Chl:C ratio (P1.0 formulation). The definition of the parameters and their default values are presented in Table 2.

35

Definition	Equation
Nitrate source minus sink	$sms(\text{NO}_3) = \lambda_{\text{NH}_4} \cdot \text{NH}_4 - \frac{L_{\text{NO}_3}}{L_N} \cdot \text{uptake}$
Ammonium source minus sink	$sms(\text{NH}_4) = -\lambda_{\text{NH}_4} \cdot \text{NH}_4 - \frac{L_{\text{NH}_4}}{L_N} \cdot \text{uptake} + \lambda_{\text{DOM}} \cdot \text{DOM}$ $+ f_n \cdot (\delta \cdot \text{uptake} + \lambda_Z \cdot Z_N + \lambda_D \cdot D_N)$
Phytoplankton source minus sink	$sms(P_N) = (1 - \delta) \cdot \text{uptake} - G_P - m_P \cdot P_N$
Zooplankton source minus sink	$sms(Z_N) = a_Z \cdot (G_P + G_D) - m_Z \cdot Z_N^2 - \lambda_Z \cdot Z_N$
Detritus source minus sink	$sms(D_N) = m_P \cdot P_N + f_Z \cdot m_Z \cdot Z_N^2 + (1 - a_Z) \cdot (G_P + G_D) - G_D - \lambda_D \cdot D_N - w_D$
DOM source minus sink	$sms(\text{DOM}) = (1 - f_n) \cdot (\delta \cdot \text{uptake} + \lambda_Z \cdot Z_N + \lambda_D \cdot D_N) - \lambda_{\text{DOM}} \cdot \text{DOM}$
Nitrogen uptake	$\text{uptake} = \mu_m \cdot L_N \cdot L_I \cdot P_N$
Light limitation	$L_I = \left[ 1 - e^{\left( -\frac{\alpha \cdot R_{\text{Chl:C}} \cdot \text{PAR}}{\mu_m} \right)} \right]$
Nutrient limitation	$L_N = L_{\text{NO}_3} + L_{\text{NH}_4}$
Nitrate limitation	$L_{\text{NO}_3} = \frac{\text{NO}_3}{K_{\text{NO}_3} + \text{NO}_3} \cdot e^{-\psi \cdot \text{NH}_4}$
Ammonium limitation	$L_{\text{NH}_4} = \frac{\text{NH}_4}{K_{\text{NH}_4} + \text{NH}_4}$
Grazing on phytoplankton	$G_P = g \cdot \frac{p \cdot P_N}{K_g + p \cdot P_N + (1-p) \cdot D_N} \cdot Z_N$
Grazing on detritus	$G_D = g \cdot \frac{(1-p) \cdot D_N}{K_g + p \cdot P_N + (1-p) \cdot D_N} \cdot Z_N$
Grazing preference for phytoplankton	$p = \frac{\tilde{p} \cdot P_N}{\tilde{p} \cdot P_N + (1-\tilde{p}) \cdot D_N}$

Table 2: Parameters of the LOBSTER model, with default values from previous studies (Lévy et al., 2005; Kremer et al., 2009).

Symbol	Definition	Value	Unit
<b>Nutrient-related parameters</b>			
$K_{NO_3}$	$NO_3$ half saturation constant	0.7 e-6	mmolN.m <sup>-3</sup>
$K_{NH_4}$	$NH_4$ half saturation constant	0.001 e-6	mmolN.m <sup>-3</sup>
$\psi$	Inhibition of $NO_3$ uptake by $NH_4$	3	unitless
$\lambda_{NH_4}$	$NH_4$ nitrification rate	0.05	d <sup>-1</sup>
<b>Phytoplankton growth and death</b>			
$\alpha$	Photosynthesis-irradiance (PI) initial slope	1.82	d <sup>-1</sup> .W <sup>-1</sup> .m <sup>2</sup> .gC.gChl <sup>-1</sup>
$\mu_m$	Maximal growth rate of phytoplankton	1	d <sup>-1</sup>
$\delta$	Excretion ratio of phytoplankton	0.05	unitless
$m_P$	Phytoplankton mortality rate	0.05	d <sup>-1</sup>
<b>Zooplankton grazing and mortality</b>			
$K_g$	Grazing half saturation constant	1 e-6	mmolN.m <sup>-3</sup>
$g$	Maximal zooplankton grazing rate	0.8	d <sup>-1</sup>
$a_Z$	Assimilated food fraction	0.7	unitless
$\lambda_Z$	Exsudation rate of zooplankton	0.07	d <sup>-1</sup>
$m_Z$	Zooplankton mortality rate	0.12 e+6	d <sup>-1</sup> .mmolN <sup>-1</sup> .m <sup>3</sup>
$\tilde{p}$	Zooplankton preference for detritus	0.8	unitless
$f_Z$	Fraction of slow sinking mortality	0.5	unitless
<b>Remineralization</b>			
$\lambda_{DOM}$	Remineralization rate of DOM	0.006	d <sup>-1</sup>
$f_n$	$NH_4$ /DOM redistribution ratio	0.75	unitless
$w_D$	Detritus sedimentation speed	3	m.d <sup>-1</sup>
$\lambda_D$	Remineralization rate of detritus	0.05	d <sup>-1</sup>

Table 4: Equations of the different phytoplankton growth formulations. P1.0: Redfield formulation with constant Chl:C ratio. P1.5: Redfield formulation with diagnostic Chl:C ratio. P2.5: Cell-quota formulation with diagnostic Chl:C ratio. P3.0/GP3.0: Cell-quota formulation with prognostic Chl:C ratio. The definition of the parameters and their default values are presented in Tables 2 and 5. Source minus sink functions (*sms*) are only for prognostic variables (in bold).

Model(s)	Definition	Equation
P1.0	Phytoplanktonic nitrogen	<b><math>sms(P_N) = (1 - \delta).uptake - G_P - m_P.P_N</math></b>
	Phytoplanktonic carbon	$P_C = R_{C:N}.P_N$
	Chlorophyll	$P_{Chl} = R_{Chl:C}.P_C$
	Nitrogen uptake	$uptake = \mu_m.L_N.L_I.P_N$
	Primary production	$prod = R_{C:N}.uptake$
P1.5	Phytoplanktonic nitrogen	<b><math>sms(P_N) = (1 - \delta).uptake - G_P - m_P.P_N</math></b>
	Phytoplanktonic carbon	$P_C = R_{C:N}.P_N$
	Chlorophyll	$P_{Chl} = \left( R_{Chl:C}^{Min} + \frac{(R_{Chl:C}^{Max} - R_{Chl:C}^{Min}).2.\mu_m.L_N}{2.\mu_m.L_N + (R_{Chl:C}^{Max} - R_{Chl:C}^{Min}).\alpha.PAR} \right) .P_C$
	Nitrogen uptake	$uptake = \mu_m.L_N.L_I.P_N$
	Primary production	$prod = R_{C:N}.uptake$
P2.5	Phytoplanktonic nitrogen	<b><math>sms(P_N) = (1 - \delta).uptake - G_P - m_P.P_N</math></b>
	Phytoplanktonic carbon	<b><math>sms(P_C) = prod - \zeta.uptake - G_P.\frac{P_C}{P_N} - m_P.P_C</math></b>
	Chlorophyll	$P_{Chl} = \left( R_{Chl:C}^{Min} + \frac{(R_{Chl:C}^{Max} - R_{Chl:C}^{Min}).2.\mu_m.L_N}{2.\mu_m.L_N + (R_{Chl:C}^{Max} - R_{Chl:C}^{Min}).\alpha.PAR} \right) .P_C$
	Nitrogen uptake	$uptake = \rho_m.L_Q^N.L_N.P_C$
	Primary production	$prod = \mu_m.L_Q^I.L_I.P_C$
	Quota-limitation of uptake	$L_Q^N = \left( \frac{Q_{max} - Q}{Q_{max} - Q_0} \right)^n$
	Quota-limitation of prod.	$L_Q^I = \frac{Q - Q_0}{Q_{max} - Q_0}$
P3.0	Phytoplanktonic nitrogen	<b><math>sms(P_N) = (1 - \delta).uptake - G_P - m_P.P_N</math></b>
GP3.0	Phytoplanktonic carbon	<b><math>sms(P_C) = prod - \zeta.uptake - G_P.\frac{P_C}{P_N} - m_P.P_C</math></b>
	Chlorophyll sms	<b><math>sms(P_{Chl}) = prod_{Chl} - G_P.\frac{P_{Chl}}{P_N} - m_P.P_{Chl}</math></b>
	Nitrogen uptake	$uptake = \rho_m.L_Q^N.L_N.P_C$
	Primary production	$prod = \mu_m.L_Q^I.L_I.P_C$
	Chlorophyll production	$prod_{Chl} = \frac{R_{Chl:N}.14}{\alpha.PAR.P_{Chl}}.prod.uptake$
	Quota-limitation of uptake	$L_Q^N = \left( \frac{Q_{max} - Q}{Q_{max} - Q_0} \right)^n$
	Quota-limitation of prod.	$L_Q^I = \frac{Q - Q_0}{Q_{max} - Q_0}$

Table 5: Parameters of the different phytoplankton growth formulations and associated default values from Geider et al. (1998).

Symbol	Definition	Default	Unit	Models
<b>Constant ratios</b>				
$R_{Chl:C}$	Chlorophyll:Carbon ratio	1/60	gChl.gC <sup>-1</sup>	P1.0
$R_{C:N}$	Phytoplankton C:N Redfield ratio	6.56	molC.molN <sup>-1</sup>	P1.0 P1.5
<b>Diagnostic chlorophyll</b>				
$R_{Chl:C}^{Min}$	Minimum Chl:C ratio	1/200	mgChl.mmolC <sup>-1</sup>	P1.5 P2.5
$R_{Chl:C}^{Max}$	Maximum Chl:C ratio	1/30	mgChl.mmolC <sup>-1</sup>	P1.5 P2.5
<b>Nutrient uptake</b>				
$\rho_m$	Maximum uptake rate (defined by $\rho_m = \mu_m \cdot Q_{max}$ )	0.2	molN.molC <sup>-1</sup> .d <sup>-1</sup>	P2.5 P3.0
$\zeta$	Cost of nitrogen assimilation	3	mol C.mol N <sup>-1</sup>	P2.5 P3.0
<b>Phytoplanktonic cell quotas</b>				
$Q_0$	Minimum value of $Q$	1/20	mol N.mol C <sup>-1</sup>	P2.5 P3.0
$Q_{max}$	Maximum value of $Q$	1/5	mol N.mol C <sup>-1</sup>	P2.5 P3.0
$n$	Shape factor	1	-	P2.5 P3.0
<b>Chlorophyll synthesis</b>				
$R_{Chl:N}^{Max}$	Maximum Chl:N ratio	2	gChl.gN <sup>-1</sup>	P3.0

Table 7: Parameter range allowed for optimization. Each parameter was binary coded on 6 bits (and had then 64 possible values).

Parameter	Lower bound	Upper bound	Increment
$\alpha$	0.3	12.9	0.2
$\mu_m$	0.1	6.4	0.1
$K_g$	1.0e-7	32.5e-7	0.5e-7
$g$	0.1	6.4	0.1
$\zeta$	1.00	4.15	0.05
$R_{Chl:N}^{Max}$	0.1	6.4	0.1

Table 8: Optimized parameters and associated cost functions ( $F$ ).

Parameter	Default values	Optimized values				
		P1.0	P1.5	P2.5	P3.0	GP3.0
$\alpha$	1.82	1.7	1.1	2.3	1.7	2.1
$\mu_m$	1	0.3	0.6	1.0	1.7	0.6
$K_g$	10.0e-7	23.0e-7	18.0e-7	22.5e-7	23.0e-7	26.0e-7
$g$	0.8	5.0	4.2	5.1	5.3	5.1
$\zeta$	3.00	-	-	3.52	3.24	3.36
$R_{Chl:N}^{Max}$	3	-	-	-	6.4	5.6
$F$ after optimization		0.855	0.823	0.790	0.802	0.773
$F$ with default value		1.118	1.217	1.1217	1.120	1.052

Table 9: Total productions, new production, and f-ratio (new production/total production in nitrogen) simulated at BATS in 1998 after optimization.

Annual values				
Model	Total Production ( $molC/m^2$ )	Total Production ( $molN/m^2$ )	New Production ( $molN/m^2$ )	f-ratio
P1.0	2.495	0.380	0.126	0.33
P1.5	2.647	0.403	0.133	0.33
P2.5	3.903	0.415	0.163	0.39
P3.0	3.728	0.421	0.134	0.32
GP3.0	3.970	0.399	0.135	0.34

Bloom period (Mars to April)				
Model	Total Production ( $molC/m^2$ )	Total Production ( $molN/m^2$ )	New Production ( $molN/m^2$ )	f-ratio
P1.0	0.855	0.130	0.064	0.49
P1.5	1.014	0.154	0.076	0.49
P2.5	1.292	0.143	0.062	0.43
P3.0	1.309	0.153	0.073	0.48
GP3.0	1.240	0.136	0.066	0.48

Oligotrophic period (July to August)				
Model	Total Production ( $molC/m^2$ )	Total Production ( $molN/m^2$ )	New Production ( $molN/m^2$ )	f-ratio
P1.0	0.424	0.064	0.016	0.25
P1.5	0.403	0.061	0.012	0.20
P2.5	0.678	0.069	0.017	0.25
P3.0	0.605	0.066	0.013	0.20
GP3.0	0.725	0.071	0.019	0.27



614 **References**

- 615 Allen, J., Somerfield, P., Siddorn, J., 2002. Primary and bacterial production in  
616 the mediterranean sea: a modelling study. *Journal of Marine Systems* 33-34,  
617 473–495.
- 618 Allen, J.I., Aiken, J., Anderson, T.R., Buitenhuis, E., Cornell, S., Geider, R.J.,  
619 Haines, K., Hirata, T., Holt, J., Le Quéré, C., Hardman-Mountford, N., Ross,  
620 O.N., Sinha, B., While, J., 2010. Marine ecosystem models for earth systems  
621 applications: The marQUEST experience. *J. Mar. Sys.* 81, 19–33. Symposium  
622 on Advances in Marine Ecosystem Modelling Research, Plymouth, England, Jun  
623 23-26, 2008.
- 624 Allen, J.I., Fulton, E.A., 2010. Top-down, bottom-up or middle-out? avoiding ex-  
625 traneous detail and over-generality in marine ecosystem models. *Prog. Oceanogr.*  
626 84, 129–133.
- 627 Allen, J.I., Polimene, L., 2011. Linking physiology to ecology: towards a new  
628 generation of plankton models. *J. Plankton Res.* 33, 989–997.
- 629 Anderson, T., 2005. Plankton functional type modelling: running before we can  
630 walk? *J. Plankton Res.* 27, 1073–1081.
- 631 Anderson, T.R., 2010. Progress in marine ecosystem modelling and the “unrea-  
632 sonable effectiveness of mathematics”. *J. Mar. Sys.* 81, 4–11. Symposium on  
633 Advances in Marine Ecosystem Modelling Research, Plymouth, England, Jun  
634 23-26, 2008.
- 635 Aumont, O., Bopp, L., 2006. Globalizing results from ocean in situ iron fertilization  
636 studies. *Global Biogeochemical Cycles* 20(2), doi:10.1029/2005GB002591.

- 637 Ayata, S.D., Lévy, M., Aumont, O., Resplandy, L., Tagliabue, A., Sciandra, A.,  
638 Bernard, O., . Variable phytoplanktonic c:n ratio decreases the variability of  
639 primary production in the ocean compared to redfield formulation. in prep. .
- 640 Bagniewski, W., Fennel, K., Perry, M.J., D'Asaro, E.A., 2011. Optimizing models  
641 of the North Atlantic spring bloom using physical, chemical and bio-optical  
642 observations from a Lagrangian float. *Biogeosciences* 8, 1291–1307.
- 643 Baklouti, M., Diaz, F., Pinazo, C., Faure, V., Queguiner, B., 2006. Investigation  
644 of mechanistic formulations depicting phytoplankton dynamics for models of  
645 marine pelagic ecosystems and description of a new model. *Prog. Oceanogr.* 71,  
646 1–33.
- 647 Baumert, H.Z., Petzoldt, T., 2008. The role of temperature, cellular quota and  
648 nutrient concentrations for photosynthesis, growth and light-dark acclimation  
649 in phytoplankton. *Limnologia* 38, 313–326.
- 650 Bernard, O., 2011. Hurdles and challenges for modelling and control of microalgae  
651 for CO<sub>2</sub> mitigation and biofuel production. *J. Process Contr.* 21, 1378–1389.
- 652 Bissett, W., Walsh, J., Dieterle, D., Carder, K., 1999. Carbon cycling in the upper  
653 waters of the Sargasso Sea: I. numerical simulation of differential carbon and  
654 nitrogen fluxes. *Deep-Sea Research I* 46, 205–269.
- 655 Blackford, J., Allen, J., Gilbert, F., 2004. Ecosystem dynamics at six contrasting  
656 sites: a generic modelling study. *J. Mar. Sys.* 52, 191–215.
- 657 Bougaran, G., Bernard, O., Sciandra, A., 2010. Modeling continuous cultures of  
658 microalgae colimited by nitrogen and phosphorus. *J. Theor. Biol.* 265, 443–454.
- 659 Carroll, D., 1996. Chemical laser modeling with genetic algorithms. *AIAA J.* 34,  
660 338–346.

- 661 Cloern, J., Grenz, C., Vidregar-Lucas, L., 1995. An empirical model of the phyto-  
662 plankton chlorophyll:carbon ratio - the conversion factor between productivity  
663 and growth rate. *Limnol. Oceanogr.* 40, 1313–1321.
- 664 Cotner, J., Ammerman, J., Peele, E., Bentzen, E., 1997. Phosphorus-limited  
665 bacterioplankton growth in the Sargasso Sea. *Aquat. Microb. Ecol.* 13, 141–  
666 149.
- 667 Dearman, J., Taylor, A., Davidson, K., 2003. Influence of autotroph model com-  
668 plexity on simulations of microbial communities in marine mesocosms. *Mar.*  
669 *Ecol. Prog. Ser.* 250, 13–28.
- 670 Doney, S., Glover, D., Najjar, R., 1996. A new coupled, one-dimensional biological-  
671 physical model for the upper ocean: Applications to the JGOFS Bermuda At-  
672 lantic time-series study (BATS) site. *Deep-Sea Research I* 43, 591–624.
- 673 Droop, M., 1968. Vitamin B12 and Marine Ecology. IV. The Kinetics of Uptake,  
674 Growth and Inhibition in *Monochrysis lutheri*. *J. Mar. Biol. Assoc. UK* 48,  
675 689–733.
- 676 Droop, M., 1983. 25 years of algal growth kinetics: a personal view. *Bot. Mar.* 26,  
677 99–112.
- 678 Dutkiewicz, S., Follows, M.J., Bragg, J.G., 2009. Modeling the coupling  
679 of ocean ecology and biogeochemistry. *Global Biogeochemical Cycles* 23,  
680 doi:10.1029/2008GB003405.
- 681 Evans, G., 2003. Defining misfit between biogeochemical models and data sets. *J.*  
682 *Mar. Sys.* 40, 49–54. 33rd International Liege Colloquium on Ocean Dynamics,  
683 Liège, Belgium, May 07-11, 2001.

- 684 Fasham, M., Ducklow, H., McKelvie, S., 1990. A nitrogen-based model of plankton  
685 dynamics in the ocean mixed layer. *J. Mar. Res.* 48, 591–639.
- 686 Faugeras, B., Bernard, O., Sciandra, A., Lévy, M., 2004. A mechanistic modelling  
687 and data assimilation approach to estimate the carbon/chlorophyll and car-  
688 bon/nitrogen ratios in a coupled hydrodynamical-biological model. *Non-Linear*  
689 *Proc. Geophys.* 11, 515–533.
- 690 Faugeras, B., Lévy, M., Memery, L., Verron, J., Blum, J., Charpentier, I., 2003.  
691 Can biogeochemical fluxes be recovered from nitrate and chlorophyll data? A  
692 case study assimilating data in the Northwestern Mediterranean Sea at the  
693 JGOFS-DYFAMED station. *J. Mar. Sys.* 40, 99–125. 33rd International Liege  
694 Colloquium on Ocean Dynamics, Liège, Belgium, May 07-11, 2001.
- 695 Fennel, K., Losch, M., Schroter, J., Wenzel, M., 2001. Testing a marine ecosystem  
696 model: sensitivity analysis and parameter optimization. *J. Mar. Sys.* 28, 45–63.
- 697 Flynn, K., 2003a. Do we need complex mechanistic photoacclimation models for  
698 phytoplankton? *Limnol. Oceanogr.* 48, 2243–2249.
- 699 Flynn, K., 2003b. Modelling multi-nutrient interactions in phytoplankton; balanc-  
700 ing simplicity and realism. *Prog. Oceanogr.* 56, 249–279.
- 701 Flynn, K., Flynn, K., 1998. The release of nitrite by marine dinoflagellates-  
702 development of a mathematical simulation. *MARINE BIOLOGY* 130, 455–470.
- 703 Flynn, K., Marshall, H., Geider, R., 2001. A comparison of two N-irradiance  
704 interaction models of phytoplankton growth. *Limnol. Oceanogr.* 46, 1794–1802.
- 705 Flynn, K.J., 2008. Use, abuse, misconceptions and insights from quota models -  
706 the Droop cell quota model 40 years on. *Oceanogr. Mar. Biol.* 46, 1–23.

- 707 Flynn, K.J., 2010. Ecological modelling in a sea of variable stoichiometry: Dys-  
708 functionality and the legacy of Redfield and Monod. *Prog. Oceanogr.* 84, 52–65.
- 709 Follows, M.J., Dutkiewicz, S., Grant, S., Chisholm, S.W., 2007. Emergent bio-  
710 geography of microbial communities in a model ocean. *Science* 315, 1843–1846.
- 711 Franks, P.J.S., 2009. Planktonic ecosystem models: perplexing parameterizations  
712 and a failure to fail. *J. Plankton Res.* 31, 1299–1306.
- 713 Friedrichs, M.A.M., Dusenberry, J.A., Anderson, L.A., Armstrong, R.A., Chai, F.,  
714 Christian, J.R., Doney, S.C., Dunne, J., Fujii, M., Hood, R., McGillicuddy, Jr.,  
715 D.J., Moore, J.K., Schartau, M., Spitz, Y.H., Wiggert, J.D., 2007. Assessment of  
716 skill and portability in regional marine biogeochemical models: Role of multiple  
717 planktonic groups. *J. Geophys. Res.-Oceans* 112.
- 718 Friedrichs, M.A.M., Hood, R.R., Wiggert, J.D., 2006. Ecosystem model complexity  
719 versus physical forcing: Quantification of their relative impact with assimilated  
720 Arabian Sea data. *Deep-Sea Research I* 53, 576–600.
- 721 Geider, R., MacIntyre, H., Kana, T., 1996. A dynamic model of photoadaptation  
722 in phytoplankton. *Limnol. Oceanogr.* 41, 1–15.
- 723 Geider, R., MacIntyre, H., Kana, T., 1998. A dynamic regulatory model of phyto-  
724 planktonic acclimation to light, nutrients, and temperature. *Limnol. Oceanogr.*  
725 43, 679–694.
- 726 Geider, R., Platt, T., 1986. A mechanistic model of photoadaptation in microalgae.  
727 *Mar. Ecol. Prog. Ser.* 30, 85–92.
- 728 Hurtt, G., Armstrong, R., 1996. A pelagic ecosystem model calibrated with BATS  
729 data. *Deep-Sea Research I* 43, 653–683.

- 730 Hurtt, G., Armstrong, R., 1999. A pelagic ecosystem model calibrated with BATS  
731 and OWSI data. *Deep-Sea Research I* 46, 27–61.
- 732 Hutchins, D.A., Mulholland, M.R., Fu, F., 2009. Nutrient Cycles and Marine  
733 Microbes in a CO<sub>2</sub>-Enriched Ocean. *Oceanography* 22, 128–145.
- 734 Jolliff, J.K., Kindle, J.C., Shulman, I., Penta, B., Friedrichs, M.A.M., Helber, R.,  
735 Arnone, R.A., 2009. Summary diagrams for coupled hydrodynamic-ecosystem  
736 model skill assessment. *J. Mar. Sys.* 76, 64–82.
- 737 Klausmeier, C., Litchman, E., Levin, S., 2004. Phytoplankton growth and stoi-  
738 chiometry under multiple nutrient limitation. *Limnol. Oceanogr.* 49, 1463–1470.
- 739 Kortzinger, A., Koeve, W., Kahler, P., Mintrop, L., 2001. C:N ratios in the mixed  
740 layer during the productive season in the northeast Atlantic Ocean. *Deep-Sea*  
741 *Research I* 48, 661–688.
- 742 Kremer, A.S., Lévy, M., Aumont, O., Reverdin, G., 2009. Impact of the subtrop-  
743 ical mode water biogeochemical properties on primary production in the North  
744 Atlantic: New insights from an idealized model study. *J. Geophys. Res.-Oceans*  
745 114, C07019, doi:10.1029/2008JC005161.
- 746 Kriest, I., Khatiwala, S., Oschlies, A., 2010. Towards an assessment of simple  
747 global marine biogeochemical models of different complexity. *Prog. Oceanogr.*  
748 86, 337–360.
- 749 Lancelot, C., Hannon, E., Becquevort, S., Veth, C., De Baar, H., 2000. Modeling  
750 phytoplankton blooms and carbon export production in the Southern Ocean:  
751 dominant controls by light and iron in the Atlantic sector in Austral spring  
752 1992. *Deep-Sea Research I* 47, 1621–1662.

- 753 Le Quéré, C., Harrison, S., Prentice, I., Buitenhuis, E., Aumont, O., Bopp, L.,  
754 Claustre, H., Da Cunha, L., Geider, R., Giraud, X., Klaas, C., Kohfeld, K.,  
755 Legendre, L., Manizza, M., Platt, T., Rivkin, R., Sathyendranath, S., Uitz, J.,  
756 Watson, A., Wolf-Gladrow, D., 2005. Ecosystem dynamics based on plankton  
757 functional types for global ocean biogeochemistry models. *GLOBAL CHANGE*  
758 *BIOLOGY* 11, 2016–2040.
- 759 Lefèvre, N., Taylor, A., Gilbert, F., Geider, R., 2003. Modeling carbon to nitrogen  
760 and carbon to chlorophyll *a* ratios in the ocean at low latitudes: Evaluation of  
761 the role of physiological plasticity. *Limnol. Oceanogr.* 48, 1796–1807.
- 762 Lévy, M., Gavart, M., Memery, L., Caniaux, G., Paci, A., 2005. A four-dimensional  
763 mesoscale map of the spring bloom in the northeast Atlantic (POMME exper-  
764 iment): Results of a prognostic model. *J. Geophys. Res.-Oceans* 110, C07S21,  
765 doi:10.1029/2004JC002588.
- 766 Lévy, M., Iovino, D., Resplandy, L., Klein, P., Madec, G., Treguier, A.M., Mas-  
767 son, S., Takahashi, K., 2012. Large-scale impacts of submesoscale dynamics  
768 on phytoplankton : local and remote effects. *Ocean Modelling* 43-44, 77–93.  
769 doi:10.1016/j.ocemod.2011.12.003.
- 770 Lévy, M., Memery, L., Madec, G., 1998. The onset of a bloom after deep winter  
771 convection in the northwestern Mediterranean sea: mesoscale process study with  
772 a primitive equation models. *J. Mar. Sys.* 16, 7–21. 28th International Liege  
773 Colloquium on Ocean Hydrodynamics, Liège, Belgium, May 06-10, 1996.
- 774 Lipschultz, F., 2001. A time-series assessment of the nitrogen cycle at BATS.  
775 *Deep-Sea Research I* 48, 1897–1924.
- 776 Mairet, F., Bernard, O., Masci, P., Lacour, T., Sciandra, A., 2011. Modelling

- 777 neutral lipid production by the microalga *Isochrysis aff. galbana* under nitrogen  
778 limitation. *Bioresource Technol.* 102, 142–149.
- 779 Matear, R., 1995. Parameter optimization and analysis of ecosystem models using  
780 simulated annealing : A case study at Station P. *J. Mar. Res.* 53, 571–607.
- 781 McGillicuddy, D., Anderson, L., Doney, S., Maltrud, M., 2003. Eddy-driven  
782 sources and sinks of nutrients in the upper ocean: Results from a 0.1 de-  
783 grees resolution model of the North Atlantic. *Global Biogeochemical Cycles*  
784 17, doi:10.1029/2002GB001987.
- 785 Michaels, A., Knap, A., 1996. Overview of the US JGOFS Bermuda Atlantic  
786 Time-series Study and the Hydrostation S program. *Deep-Sea Research I* 43,  
787 157–198.
- 788 Mitra, A., Flynn, K.J., Fasham, M.J.R., 2007. Accounting for grazing dynamics in  
789 nitrogen-phytoplankton-zooplankton models. *Limnol. Oceanogr.* 52, 649–661.
- 790 Mongin, M., Nelson, D., Pondaven, P., Brzezinski, M., Treguer, P., 2003. Simula-  
791 tion of upper-ocean biogeochemistry with a flexible-composition phytoplankton  
792 model: C, N and Si cycling in the western Sargasso Sea. *Deep-Sea Research I*  
793 50, 1445–1480.
- 794 Monod, J., 1949. The growth of bacterial cultures. *Annu. Rev. Microbiol.* 3,  
795 371–394.
- 796 Monod, J., 1950. La technique de culture continue théorie et applications. *Ann.*  
797 *I. Pasteur Paris* 79, 390–410.
- 798 Moore, J., Doney, S., Kleypas, J., Glover, D., Fung, I., 2002. An intermediate  
799 complexity marine ecosystem model for the global domain. *Deep-Sea Research*  
800 *I* 49, 403–462.



- 801 Oschlies, A., 2002. Can eddies make ocean deserts bloom? *Global Biogeochemical*  
802 *Cycles* 16, doi:10.1029/2001GB001830.
- 803 Oschlies, A., Schartau, M., 2005. Basin-scale performance of a locally optimized  
804 marine ecosystem model. *J. Mar. Res.* 63, 335–358.
- 805 Redfield, A.C., Ketchum, B.H., Richards, F.A., 1963. The influence of organisms  
806 on the composition of sea water, in: Hill, M.N. (Ed.), *The sea*. Wiley, New York,  
807 pp. 26–77.
- 808 Riebesell, U., Schulz, K.G., Bellerby, R.G.J., Botros, M., Fritsche, P., Meyerhoefer,  
809 M., Neill, C., Nondal, G., Oschlies, A., Wohlers, J., Zoellner, E., 2007. Enhanced  
810 biological carbon consumption in a high CO<sub>2</sub> ocean. *Nature* 450, 545–548.
- 811 Ross, O.N., Geider, R.J., 2009. New cell-based model of photosynthesis and photo-  
812 acclimation: accumulation and mobilisation of energy reserves in phytoplankton.  
813 *Mar. Ecol. Prog. Ser.* 383, 53–71.
- 814 Salihoglu, B., Garcon, V., Oschlies, A., Lomas, M.W., 2008. Influence of nutri-  
815 ent utilization and remineralization stoichiometry on phytoplankton species and  
816 carbon export: A modeling study at BATS. *Deep-Sea Research I* 55, 73–107.
- 817 Sambrotto, R., Savidge, G., Robinson, C., Boyd, P., Takahashi, T., Karl, D., Lang-  
818 don, C., Chipman, D., Marra, J., Codispoti, L., 1993. Elevated consumption of  
819 carbon relative to nitrogen in the surface oceans. *Nature* 363, 248–250.
- 820 Schartau, M., Oschlies, A., 2003. Simultaneous data-based optimization of a 1D-  
821 ecosystem model at three locations in the North Atlantic: Part I - Method and  
822 parameter estimates. *J. Mar. Res.* 61, 765–793.

- 823 Schartau, M., Oschlies, A., Willebrand, J., 2001. Parameter estimates of a zero-  
824 dimensional ecosystem model applying the adjoint method. *Deep-Sea Research*  
825 I 48, 1769–1800.
- 826 Sciandra, A., 1991. Coupling and uncoupling between nitrate uptake and growth  
827 rate in *Prorocentrum minimum* (Dinophyceae) under different frequencies of  
828 pulsed nitrate supply. *Mar. Ecol. Prog. Ser.* 72, 261–269.
- 829 Smith, S.L., Yamanaka, Y., 2007. Quantitative comparison of photoacclimation  
830 models for marine phytoplankton. *Ecological Modelling* 201, 547–552.
- 831 Spitz, Y., Moisan, J., Abbott, M., 2001. Configuring an ecosystem model using  
832 data from the Bermuda Atlantic Time Series (BATS). *Deep-Sea Research I* 48,  
833 1733–1768.
- 834 Spitz, Y., Moisan, J., Abbott, M., Richman, J., 1998. Data assimilation and a  
835 pelagic ecosystem model: parameterization using time series observations. *J.*  
836 *Mar. Sys.* 16, 51–68. 28th International Liege Colloquium on Ocean Hydrody-  
837 namics, Liège, Belgium, May 06-10, 1996.
- 838 Steinberg, D., Carlson, C., Bates, N., Johnson, R., Michaels, A., Knap, A., 2001.  
839 Overview of the US JGOFS Bermuda Atlantic Time-series Study (BATS): a  
840 decade-scale look at ocean biology and biogeochemistry. *Deep-Sea Research I*  
841 48, 1405–1447.
- 842 Stow, C.A., Jolliff, J., McGillicuddy, Jr., D.J., Doney, S.C., Allen, J.I., Friedrichs,  
843 M.A.M., Rose, K.A., Wallhead, P., 2009. Skill assessment for coupled biologi-  
844 cal/physical models of marine systems. *J. Mar. Sys.* 76, 4–15.
- 845 Tagliabue, A., Arrigo, K., 2005. Iron in the Ross Sea: 1. Impact on CO<sub>2</sub> fluxes via

- 846 variation in phytoplankton functional group and non-Redfield stoichiometry. *J.*  
847 *Geophys. Res.-Oceans* 110, doi:10.1029/2004JC002531.
- 848 Tagliabue, A., Bopp, L., Gehlen, M., 2011. The response of marine car-  
849 bon and nutrient cycles to ocean acidification: Large uncertainties related to  
850 phytoplankton physiological assumptions. *Global Biogeochemical Cycles* 25,  
851 doi:10.1029/2010GB003929.
- 852 Taylor, K., 2001. Summarizing multiple aspects of model performance in a single  
853 diagram. *J.Geophys. Res.* 106, 7183–7192.
- 854 Vatcheva, I., DeJong, H., Bernard, O., Mars, N.J.L., 2006. Experiment selection  
855 for the discrimination of semi-quantitative models of dynamical systems. *Artif.*  
856 *Intel.* 170, 472–506.
- 857 Vichi, M., Masina, S., 2009. Skill assessment of the pelagos global ocean biogeo-  
858 chemistry model over the period 19802000. *Biogeosciences* 6, 2333–2353.
- 859 Vichi, M., Masina, S., Navarra, A., 2007. A generalized model of pelagic bio-  
860 geochemistry for the global ocean ecosystem. part ii: numerical simulations.  
861 *Journal of Marine Systems* 64(1-4), 110–134.
- 862 Vogt, M., Vallina, S.M., Buitenhuis, E., Bopp, L., Le Qur, C., 2010. Simulating  
863 dimethylsulphide seasonality with the dynamic green ocean model planktom5.  
864 *Journal of Geophysical Research - Oceans* 115(C6), C06021.
- 865 Ward, B.A., Friedrichs, M.A.M., Anderson, T.R., Oschlies, A., 2010. Parameter  
866 optimisation techniques and the problem of underdetermination in marine bio-  
867 geochemical models. *J. Mar. Sys.* 81, 34–43. Symposium on Advances in Marine  
868 Ecosystem Modelling Research, Plymouth, England, Jun 23-26, 2008.

- 869 Webb, W., Newton, M., Starr, D., 1974. Carbon dioxide exchange of *Alnus rubra*:  
870 a mathematical model. *Oecologia* 17, 281–291.
- 871 Williams, R., Follows, M., 1998. The Ekman transfer of nutrients and maintenance  
872 of new production over the North Atlantic. *Deep-Sea Research I* 45, 461–489.
- 873 Wroblewski, J., 1977. A model of phytoplankton plume formation during variable  
874 Oregon upwelling. *J. Mar. Res.* 35, 357–394.
- 875 Zonneveld, C., 1998. Light-limited microalgal growth: a comparison of modelling  
876 approaches. *Ecological Modelling* 113, 41–54. 1st European Ecological Modelling  
877 Conference, Pula, Croatia, Sep 16-19, 1997.